INTELLIGENT FEEDBACK CONTROLLER DESIGN FOR DC-DC CONVERTER

By

OWAIS KHALID

DEPARTMENT OF ELECTRICAL ENGINEERING

NATIONAL UNIVERSITY OF MODERN LANGUAGES

ISLAMABAD

July, 2025

INTELLIGENT FEEDBACK CONTROLLER DESIGN FOR DC-DC CONVERTER

By

OWAIS KHALID

Supervised By

DR. HAMMAD DILPAZIR

MS EE, National University of Modern Languages, Islamabad, 2025

A THESIS SUBMITTED IN PARTIAL FULFILMENT OF
THE REQUIREMENTS FOR THE DEGREE OF

MASTER OF SCIENCE

In **ELECTRICAL ENGINEERING**

To

DEPARTMENT OF ELECTRICAL ENGINEERING

FACULTY OF ENGINEERING & COMPUTING

NATIONAL UNIVERSITY OF MODERN LANGUAGES ISLAMABAD

THESIS AND DEFENSE APPROVAL FORM

The undersigned certify that they have read the following thesis, examined the defense, are satisfied with overall exam performance, and recommend the thesis to the Faculty of Engineering and Computing for acceptance.

Thesis Title: Intelligent Feedback Controller Design for DC-DC Converter

Submitted By: Owais Khalid **Registration #:** MS/EE/F21/11

Master of Master of Science in Electrical Engineering
Title of the Degree

Electrical Engineering
Name of Discipline

Dr. Hammad Dilpazir _____
Name of Research Supervisor Signature of Research Supervisor

Dr. Noman Malik _____
Dean (FEC) Signature of Dean (FEC)

Brig. Shahzad Munir _____
Director General Signature of Director General (FEC)

AUTHOR'S DECLARATION

I Owais Khalid

Son of Khalid Nafeez

Registration # MS/EE/F21/11

Discipline ELECTRICAL ENGINEERING

Candidate of **Master of Science in Electrical Engineering (MSEE)** at the National University of Modern Languages do hereby declare that the thesis **Intelligent Feedback Controller Design for DC-DC Converter** submitted by me in partial fulfillment of MSEE degree, is my original work, and has not been submitted or published earlier. I also solemnly declare that it shall not, in future, be submitted by me for obtaining any other degree from this or any other university or institution. I also understand that if evidence of plagiarism is found in my thesis/dissertation at any stage, even after the award of a degree, the work may be cancelled and the degree revoked.

_____
Signature of Candidate

Owais Khalid
Name of Candidate

_____
Date

ABSTRACT

Title: Intelligent Feedback Controller Design for DC-DC Converter

In this research, a feedback control system for DC-DC converter is designed using artificial intelligence. PID control is widely used as the control method for DC-DC converters. The PID parameter tuning process parameters remains hard in nonlinear case scenarios. As in such scenarios system needs to handle disturbances during load changes and operate under dynamically changing conditions. The system control response with the inclusion of AI technology leads to an improvement in the operation of DC-DC converters through their feedback system and improved the overall ripple on output line. Also, it helps the system to become more stable across different loads at the same time and achieve maximum performance. Furthermore, the proposed AI-based controller has been successfully applied to a real-time Voltage-to-Grid (70V-380V) case scenario, replacing the PID controller in a Neutral Point Clamped (NPC) converter topology. This shows the versatility and effectiveness of this control technique in complex power conversions. Replacement of AI based control with PID helps system in continuous learning and adaptation and as a result real-time control, reduction in output voltage ripple, and enhanced system adaptability under dynamic load conditions and making it suitable for current applications of DC-DC converters.

TABLE OF CONTENTS

LIST OF TABLES

LIST OF FIGURES

LIST OF ABBREVIATIONS

V2G	-	Vehicle to Grid
NPC	-	Neutral Point Clamp
DC	-	Direct Current
AC	-	Actively Clamped
SRT	-	Series Resonant Tank
BCM	-	Boundary Conduction Mode
DCM	-	Discontinuous Conduction Mode
SPT	-	State Plan Trajectory
EV	-	Electric Vehicle
AI	-	Artificial Intelligence
ANN	-	Artificial Neural Network
PID	-	Proportional-Integral-Derivative
MPC	-	Model Predictive Control
SGD	-	Sustainable Development Goal
UNDP	-	United Nations Development Programme
THD	-	Total Harmonic Distortion
RNN	-	Recurrent Neural Network
CNN	-	Convolutional Neural Network
SVM	-	Support Vector Machine
FLC	-	Fuzzy Logic Controller
FF	-	Feedforward
NEVP	-	National Electric Vehicle Policy of Pakistan
NPC	-	Neutral Point Clamped
ZVS	-	Zero Voltage Switching
HIL	-	Hardware-in-the-loop

LIST OF SYMBOLS

ω_r	-	Angular Resonance Frequency
α	-	initial phase offset at $t = t_1$ in the resonant sinusoidal waveform.
n	-	Turn ratio
t_0	-	initial time of the resonant operation
D	-	Duty cycle
ton	-	On period of switch
K_p	-	Proportional gain
K_i	-	Integral gain
K_d	-	Derivative gain
T_{sw}	-	Switching Time
L_r	-	Resonant inductance
i_{Lres}	-	Current through resonant inductor
V_{LV}	-	Primary side voltage
V_{HV}	-	Secondary side voltage
v_{Cr_1}	-	Voltage across resonant capacitor
Z_r	-	Impedance at resonance
I_{H_V}	-	Output current
I_{H_V}	-	Input current
D_F	-	Forward duty ratio
G_f	-	Forward Gain of the converter
f_{sw}	-	Switching frequency
N_p	-	Number of turns of primary side
N_s	-	Number of turns of secondary side
B_m	-	Flux Density
A_e	-	Area of core
X_{norm}	-	Normalized value

ACKNOWLEDGMENT

I would like to express my gratitude to all individuals who have contributed significantly to the completion of my thesis. First and foremost, I am deeply thankful to Allah (SWT) who has always showered his countless blessings on me. I would like to thank My supervisor, Dr. Hammad Dilpazir, for his exceptional guidance, unwavering support, and scholarly insights throughout this research journey. His mentorship has been invaluable in shaping my academic growth and refining the scope of this thesis. I extend my sincere appreciation to my Examination Committee members for their meticulous review, constructive feedback, and scholarly advice. Their expertise and thoughtful contributions have greatly enhanced the rigor and quality of this thesis.

DEDICATION

I would like to dedicate my thesis work to my beloved parents, my wife and teachers who have always supported me.

CHAPTER 1: INTRODUCTION

1.1. Background and Scope

DC-DC converters are an important part of any electronic system, since they are used for conversion of DC voltages. These are even used if the input and output voltages are nominally the same, for example 24V to 24V, a DC to DC converter is often still necessarily used. This is because real power supplies are affected by fluctuations due to load variations, battery discharge or line disturbance, causing instability in the output. DC-DC converters produce a stable and well-regulated output voltage, thus preventing damage or malfunctions to sensitive components. They further provide improved efficiency and minimized power losses as well as galvanic isolation when required, which makes them suitable for applications including among others electric vehicles, renewable energy systems, industrial automation and consumer electronics. An important characteristic of these converters is that they use feedback control, which is usually PID control. It consists of a feedback mechanism that checks the output voltage all the time against a reference stationary value. This error signal is used in real time to modify the switching duty cycle of the converter, and it allows to keep the output voltage stable, even under large variations of input or load. Embodiments of this process to be closed loop is important to the accurate functioning of DC-DC Converters and opens the way to investigation of sophisticated control methodologies, such as artificial neural networks for enhanced dynamic performance and robustness in intricate power systems [1].

DC-DC converters can be classified into two types, which are isolated and non-isolated types based on input-output electrical connectivity. Buck, Boost, and buck-boost converters are basic non-insulated converters that have a direct electrical connection between output and input. Buck is used to step down whereas Boost is for step up input voltages. Buck-Boost can do both step up or step down the input voltage. These types of converters are simpler, smaller, and cheaper but do not provide electrical isolation between input and output. Fly-back, Forward, and Push-Pull converters are the kinds of Isolated Converters that have transformers that keep input and output electrical isolated. The isolated converters can actually be push-pull converters [2]. The choice of converters depends on the specific application requirements for safety, noise immunity, size, cost, and performance.

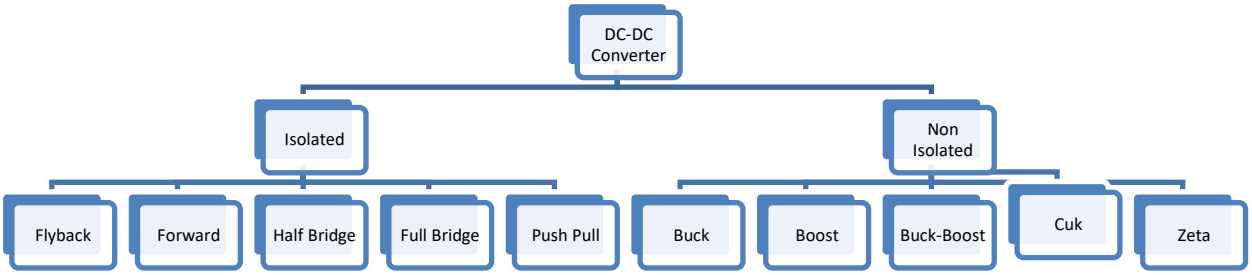

Figure 1.1: Types of DC-DC Converters

1.1.1 Significance of DC-DC Converters in EVs

Increases in both green energy sovereignty and carbon emission decrease have prompted global EV adoption to reach significant levels. The adoption of EVs has brought about the innovative platform which enables EVs to feed power back into the power grid during episodes of voltage instability together with changing power consumption patterns. The drawing and feeding of energy between the grid and vehicle are possible through V2G technology by using a DC-DC converter which works as a buck converter during G2V operations and as a boost converter during V2G operations. The electricity present in EV batteries offers vital stabilization capabilities to power grids by providing support during short-term instability occurrences. The implementation of EV batteries creates a more effective solution for managing the intermittent energy production from solar and wind resources [2]. Onboard battery chargers (OBCs) gain popularity since they let EV owners charge their vehicles through regular power outlets commonly seen in homes. These charging units encounter problems because of their restricted dimensions.

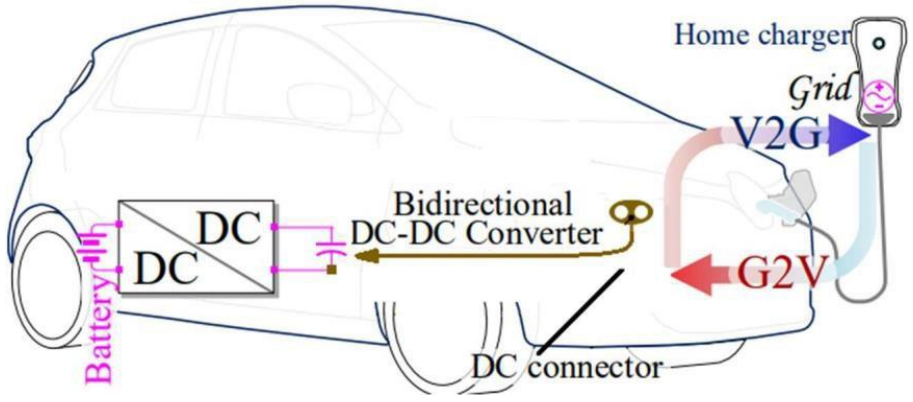

Figure 1. 2: Bi-directional power transmission between electric vehicle batteries and the power grid

Electric vehicles take part in Vehicle-to-Grid power sharing protocols to make their stored energy flow in two directions. The system permits electric vehicles to pull power from the grid for charging functions and produce grid feedback power. The power system incorporates V2G functions for backup during times when voltage instability or power deficits occur as shown in Figure 1.2. This EVs attain mobile energy storage capabilities through functional enhancements that enable connection to power grids operations.

1.1.2 Power Grid Stability:

The V2G system supports power transmission during times of low voltage which results from excessive demand. Every national power grid must keep supply levels equal to demand to achieve stable electrical voltage and frequency operations. The rising inclusion of wind turbines and photovoltaic units into power grids makes them susceptible to unpredictable power fluctuations that harm system stability. The V2G system enables EVs to act as power resources which stabilize the fluctuations between power generation and electricity demand.

1.1.3 Peak Demand Management:

The daily power requirements of electricity usage show major fluctuations because the maximum usage typically happens at particular peak times. Peak demand surges require expensive peak load plants for their management. Through V2G technology electric vehicles possess the capability to share stored energy with the power grid when energy usage reaches its peak levels. The efficient management of power usage enables better resource allocation and cuts down costs for electricity generation through the elimination of additional power production facilities.

1.1.4 Integration of Sustainable Energy Systems:

The unpredictability of wind and solar electricity generation stems from their dependency on atmospheric weather systems along with geographical location distinctive characteristics. Through the V2G system operators can solve the problem of volatile renewable energy output by storing surplus energy during high production times and sending it back to the energy network during periods of low renewable energy supply. The process takes advantage of excess renewable energy to stabilize the power grid and reduce the erratic characteristics of renewable generation thus improving both stability and efficiency.

1.1.5 Backup Power:

EVs with V2G technology embedded act as dependable standby power systems for residential, commercial and important infrastructure when severe weather or service interruptions trigger power grid outages in areas which experience regular electrical disruptions. During emergencies EV batteries can provide power for vital services until backup systems become available which builds community resistance and reduces conventional backup needs.

1.2 DC-DC Converters and Duty Cycle Control

The switching period of a buck converter can be seen at its input, this is how the performance of buck converter is defined, the duty cycle of the converter which is the ratio of life of switch (transistor) in "on" state and total switching period.

Duty cycle (D) defined as the ratio between on time and total time period ($D = \frac{ton}{T}$)

where ton is the time for which the switch is closed (conducting), and T is the total period of the switching cycle.

Working Principle: The duty cycle control of Buck converters determines their output performance since an increased duty cycle produces increased output voltage while reduced duty cycle lowers it. A Boost converter regulates output voltage by increasing the duty cycle to boost voltage but reduces voltage when decreasing the cycle. The converter controls the duty cycle with precision to stabilize output voltage levels under changing load situations.

Feedback Control: Deliver stability to the output voltage by using feedback control systems due to variations in input voltage along with changing loads. PID controllers represent a standard method to accomplish this process. The duty cycle receives changes from controllers that operate based on error signals that indicate the deviation between output target voltage and the actual measured output voltage. The modification process stabilizes system operation when it faces environmental changes.

1.2.1 Limitations of PID Control:

The dynamic systems with both non-linear properties and time-dependent elements create difficulties for controllers based on PID. Some of their limitations include:

I. The process to find proper PID parameter values (Kp, Ki, Kd) remains complex during tuning operations. The determination process becomes increasingly hard when working with systems

presenting complex dynamic conditions.

II. The response speed of PID controllers becomes inadequate when the system experiences sudden shifts in load conditions. The controller produces slower response times to transients while the output voltage displays increased fluctuations because of the input voltage changes. New advanced control methods are required due to restrictions found in systems which need better precision and adaptability.

Even though proportional-integral-derivative (PID) controllers still prevail in DC-DC converter design, recent works have uncovered three fundamental limitations that give current controllers un-satisfied results in advanced applications. Second, PID control parameter are fixed, hence cannot change based on dynamic operating conditions and this is reflected in ±5% output voltage deviation of electric vehicle charging systems during rapid load transients [3] and in similar instability for renewable energy systems [4]. The second is that PID control is intrinsically linear, which does not nullify the nonlinearities of the converter, leading to THD increased due to switching dead time effects [5] and 15-20% inductance variation from the saturation events [6]. Finally, the sensitivity of the derivative term to noise makes undesirable design compromise necessary: either lost bandwidth (50μs response delays [7]) or efficiency reducing filtering (2-3% loss in data center applications [8]). Collectively we arrive at these limitations which are the motivations for the neural network approach developed in this work.

1.2.2 Artificial Neural Networks (ANNs) as an Alternative Control Strategy

To overcome the limitations of conventional PID control, this study explores the use of Artificial Neural Networks (ANNs) for duty cycle regulation in DC-DC converters. ANNs provide several benefits that make them well-suited for this purpose:

I. The neural network regulates itself by adapting to operational changes which permits control of dynamic loads variations [9].

II. They produce good results within dynamic control systems that lack efficiency from linear control techniques [10].

III. This technology processes several inputs simultaneously which suits its operation for multiple application needs. The advanced DC-DC converter designs benefit from ANN technologies when it comes to managing systems with multiple variables.

1.2.3 Implementation of ANN for Duty Cycle Control:

The collection process involved obtaining historical records from the DC-DC converter that included its input voltage and output data and operational current measurement. Researchers collect input from voltage, load current and duty cycle values that correspond to each other. [11]

The ANN receives training through the utilization of the gathered data. The network learns to correlate. The ANN learns to associate input measurements of voltage and current readings to generate an optimal duty cycle output. Backpropagation supports the refinement of weights and biases through a learning algorithm for the network.

The implemented ANN goes into real-time control following its training process. Real-time measurements of input voltage and output voltage and load conditions feed into the system for generating optimal results. The controller requires a duty cycle computation for sustaining target output voltage level

Feedback Loop: The ANN's feedback mechanism constantly adjusts its produced outputs through real-time system state monitoring to make dynamic changes in the duty cycle when operational changes occur.

1.3 Motivation

The recent advancement of electric vehicles (EVs) provides two key functions by helping stabilize power grids through voltage control and strengthening network stability during grid instability. The Vehicle-to-Grid (V2G) technology allows EVs to store and release power which improves their dual functionality as well as provides economic benefits to their owners. The need for advanced DC-DC converters continues to grow because the power grid requires real-time autonomous management of power flow direction to integrate EVs conveniently. My research deals with a high- performance DC-DC converter dedicated for EV usage which incorporates artificial intelligence (AI) technology into its feedback control system. This AI-based system predates PID controllers by design to deliver superior operational functions and efficiency in converter management operations. The DC- DC converter requires enhanced power density capability because rising onboard charging system requirements demand it. This research implements AI as an essential part of the control framework to enhance the converter operation by ensuring dynamic responsiveness and efficiency and reliability optimization. The research addresses both present technical difficulties in the field and enhances sustainable energy solutions for transportation systems.

1.4 Justification for the Selection of Topic:

Scientific progress in power electronics technology has enabled many different kinds of power converters to become necessary components for electric vehicles to link to national power grids worldwide. The growing importance of EVs in automotive markets combined with rising popularity of DC microgrids has created a market requirement for efficient onboard converters. The main focus of my scientific inquiry involves creating an AI-powered advanced DC-DC converter that improves operational performance. The converter design aims to improve conventional power stage topologies through fewer switch components which enhances power density while making the system more simplified. AI-based feedback control systems enable the converter to detect operating changes automatically while achieving superior results beyond standard control techniques. The AI-enabled converter design upgrade brings an essential progress in improving onboard charging systems efficiency and reliability which creates greater opportunities for EV market expansion.

1.5 Problem Statement

The PID (Proportional-Integral-Derivative) controller represents one of the main feedback controls methods used for maintaining physical system behavior. Exactly-tuned proportional, integral and derivative gains are necessary to obtain best possible performance results from PID controllers. The system tuning process demands extensive work and delays the operational response of the system and no system in ideal so in non-linear systems where sudden changes can happened PID can't abruptly respond as desired as result output fluctuates and a ripple is observed at output. When PID controllers receive inaccurate parameter settings they typically produce overshooting behavior together with multiple oscillations which might destabilize the controlled system. Traditional feedback control systems operate with static control parameters since these parameters remain unaltered despite system or environmental fluctuations. System performance may experience degradation leading to instability because the control parameters reach their set limits when system variations occur. Control strategies that operate conventionally depend on static system parameters which users should know precisely. The actual operational environment introduces variable system parameters which stem from aging and wear and tear along with environmental effects. The adjusted system produces adverse effects on the control system which leads to both performance instability together with efficiency degradation. The parameter changes generally make conventional control systems prone to instability because they do not hold

stability under such conditions. The volatility of DC-DC converter conditions calls for alternative intelligent controls as more suitable solutions. The advanced techniques demonstrate effective operation when dealing with non-linearities and time delays and noise that naturally occur within DC-DC converters. These advanced techniques provide enhanced performance together with stability features along with adaptability abilities that deliver a superior solution to power conversion systems.

1.6 Objectives of the research:

I. To address the output ripple issues by analyzing the dynamic response of system.

II. To improve the overall system stability in load transients.

The dynamic response mechanism located in DC-DC converters stands central to feedback control system operation. The converter determines its reaction to abrupt system changes through the feedback control determination process. The converter output receives reference value comparison triggering an error signal from this comparison. The control signal receives modifications through the error signal generated by output voltage measurement to achieve stable output voltage.

The efficiency of this adjustment relies heavily on the converter's dynamic response. A converter with a rapid and precise dynamic response offers several advantages:

Disturbance Mitigation: It effectively removes disturbances and fluctuations in load current, in order to make sure that the output voltage remains stable and within desired limits. This stability is important in many applications that requires high-precision voltage regulation, such as power supplies for sensitive electronic devices.

Enhanced Transient Performance: A improved dynamic response removes the overshoot for changes in load or input voltage, thereby improving the converter's overall efficiency and reliability.

Component Stress Reduction: By swiftly adjusting to changes, the converter minimizes stress on components like capacitors and inductors, which might otherwise experience high voltage or current transients during load or input voltage variations.

In summary, achieving a stable, accurate, and efficient operation of DC-DC converters is essential, and the dynamic response plays a pivotal role in this process. The design of the feedback control system is crucial in attaining the desired dynamic performance.

1.7 SGD Mapping and Relevance to National Needs:

The research to improve DC-DC converter dynamics with AI-based controls combined to conventional PID functions best fulfills multiple United Nations Development Program (UNDP) Sustainable Development Goal (SDG) criteria.

One SDG that could align with this research is SDG 7: Affordable and Clean Energy represents an appropriate fit with this research contribution. The objective of this Social Development Goal is to provide everyone with obtainable dependable sustainable contemporary energy services. The proposed investigations about DC-DC converter efficiency and performance enhancement through renewable energy source use and minimized energy loss relate directly to achieving SDG targets.

Another relevant SDG could be SDG 9: Industry Innovation and Infrastructure would be relevant in this case. The SDG targets two core components: sustainable infrastructure alongside innovation and technological growth at the same time it promotes industrial advancement. Research on developing intelligent control design for DC-DC converters which predicts duty cycle would support SDG 9 through innovation and power electronics technology advancement.

These United Nations SDGs allow the proposed research to tackle crucial worldwide problems related to energy access and sustainability and product innovation. The research team should distribute its insights to stakeholders including policy makers and industry practitioners who need guidance for power electronics development alongside sustainable energy activities.

The Pakistani Government actively supports the national implementation of electric vehicles across the country. Under the established policy a 30% automobile market share stands as the target until 2030 then a 90% goal becomes active in 2040 [12]. The targets for electric two-wheelers under the policy present more ambitious goals which require achieving 50% market penetration by 2030 followed by full market dominance by 2040 as Figure 1.3 shows.

The National Electric Vehicle Policy (NEVP) has resulted in enabling existing fuel stations in Pakistan to install multiple charging stations. The policy establishes a detailed blueprint for EV production together with a nationwide expansion of charging stations in Pakistan. The development of EV chargers through local research by firms enables cost reductions which help to establish a domestic industry.

Companies such as MG and Gu-Go have introduced EVs or hybrid models, reflecting increasing interest and market opportunities in this sector. As electric vehicles gain a stronger foothold in Pakistan's automotive market, the creation of EV chargers tailored to local requirements has become essential

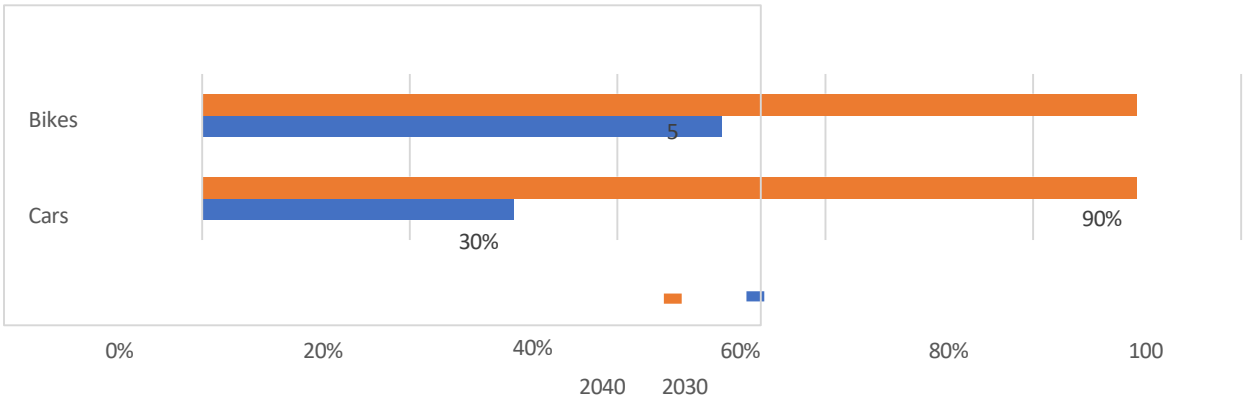

Figure 1.3: Trend of EVs in Pakistan's Automobile Market

In the future, EVs are expected to support vehicle-to-grid (V2G) operations in addition to the traditional grid-to-vehicle (G2V) charging. This dual functionality will help reduce charging expenses and contribute to grid stability. Consequently, the Pakistani automotive market will need V2G-compatible EV chargers.

1.8 Areas of Application

Application of this power converter lies in three possible schemes of the converters according to the site of installation and power levels.

- Power Outlet Chargers
- Onboard Chargers
- Fast Charging Stations

1.9 Thesis Outline

The thesis is structured to provide a comprehensive exploration of the research topic. Chapter 2 presents a detailed literature review, analyzing the advantages and disadvantages of existing topologies and how are these topologies being used in modern DC-DC converters. Chapter 3 introduces the proposed novel DC-DC converter with AI control, including detailed explanation how the dataset is gathered by simulating the DC-DC converter with PID, various modes of operation, and theoretical operational waveforms. This chapter also examines the voltage gains of the converter. Chapter 4 validates the theoretical findings through simulations and experimental results, offering a thorough comparison of performance of PID control with ANN and shows its performance on different load and transient conditions. Chapter 5 of this thesis provides research findings and identifies possible research paths for future investigations.

CHAPTER 2: LITERATURE REVIEW

2.1 General Overview of DC-DC Converters

DC-DC converters operate as power conversion devices which adjust either up or down direct (DC) voltage between input supply and output terminations. The electronic systems especially EVs rely on DC-DC converters to provide different voltage levels which different components need [13]. The overall subblocks within a DC-DC converter is shown in Figure 2.1. The functionality and design approach of DC-DC converters leads to the creation of two fundamental converter types which include non-isolated and isolated versions.

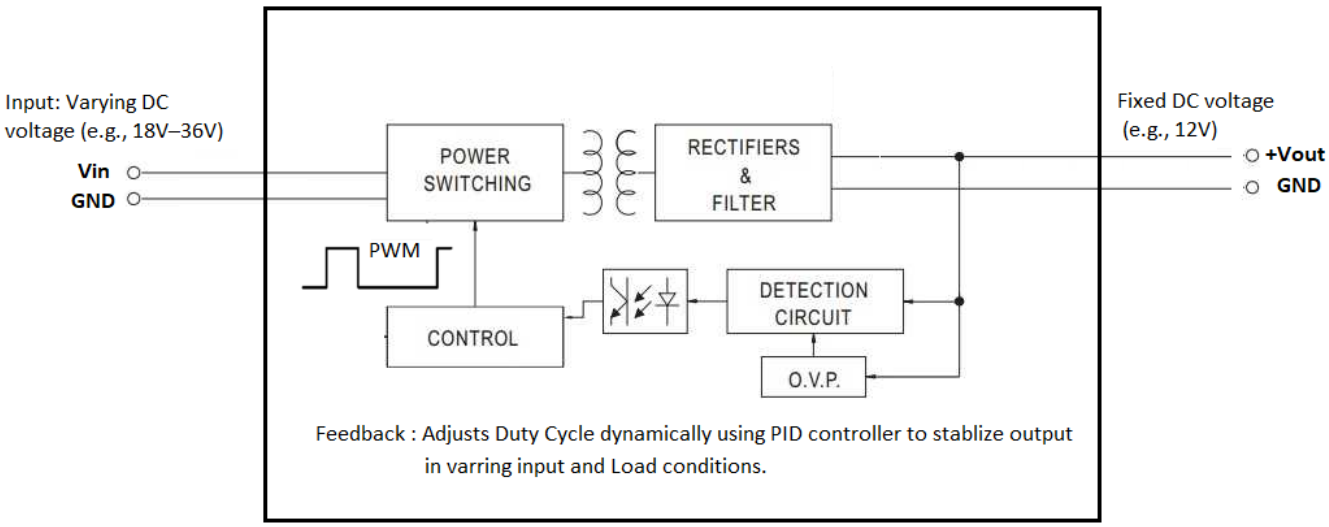

Figure 2.1: DC-DC Converter Block Diagram

2.1.1 Non-Isolated Converters:

Non-isolated DC-DC converters take non-isolated DC voltages directly from the input stage to produce a different output voltage level without adding any galvanic separation. Two stages in the converter system maintain their operating ground reference through common connection. Non-isolated converters achieve smaller size along with better cost efficiency and higher efficiency because of their simpler design [14].

2.1.2 Buck Converter:

A buck converter operates as one of the basic non-isolated power converter units which transforms higher input voltages into lower output voltages. The buck converter operates as a non-isolated power

converter which converts elevated input voltage to lower output voltage. The charging process of the inductor occurs through the input voltage during MOSFET on-states. After turning off the transistor the inductor releases energy to the load path which passes through either a freewheeling diode or a synchronous rectifier. The converter combines two fundamental components including the switching element together with an inductor and diode as well as another component which acts as a voltage filter through a capacitor. This converter functions via Continuous Conduction Mode (CCM) in addition to Discontinuous Conduction Mode (DCM) which enables inductor current to flow continuously through complete cycles and briefly become zero respectively. This converter finds practical use in mobile phone charger applications because it provides stable lower voltage outputs [14].

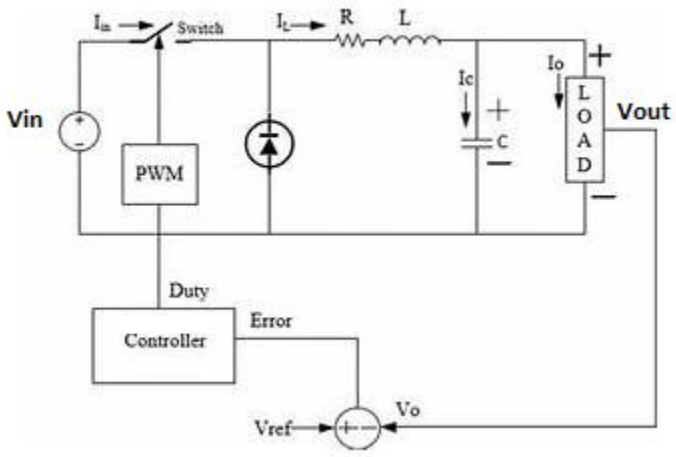

Figure 2.2: Buck Converter Circuit Diagram

2.1.3 Boost Converter:

Different from other DC-DC converters, a boost converter utilizes its three main components for the purpose of enhancing low input voltages toward increased output voltages. Boost converters need a switching transistor (MOSFET), an inductor along with a diode or synchronous rectifier in their basic structure. The inductor stores energy when the transistor is turned on and gives the stored energy to the load after the transistor switches off producing an output voltage higher than the input voltage [15]. The converter operates either in Continuous Conduction Mode (CCM) or Discontinuous Conduction Mode (DCM). Under CCM the inductor current remains above zero throughout each switching period but DCM has periods of zero current. Boost converters serve applications that need elevated output voltages specifically for LED lighting systems among others.

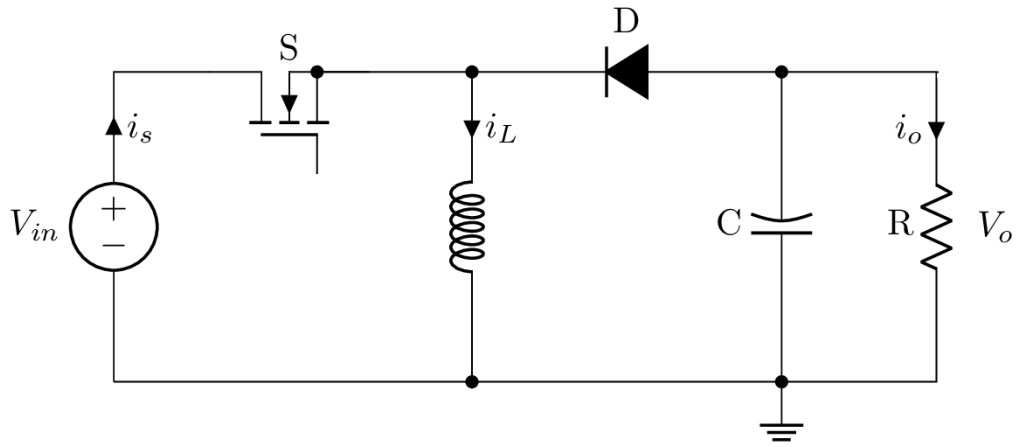

Figure 2.3: Boost Converter Circuit Diagram

2.1.4 Buck-Boost Converter:

The buck-boost converter brings together buck and boost converter capabilities to control output voltages across the whole input range from low to high levels. The converter includes a MOSFET along with an inductor and a diode or synchronous rectifier and a capacitor which functions as an output voltage filter. Buck-boost converters serve two purposes in applications which include battery-powered devices for charging as well as renewable energy systems where they stabilize voltage levels from variable sources including solar and wind energy.

2.1.5 Isolated DC-DC Converters:

The need for specifying electrical grounding between input and output requires using isolated DC-DC converters. These converters are widely used in industry because of the inherent safety feature of isolation.

2.1.6 Fly back Converter:

The fly back converter operates by storing energy in the primary side of the transformer and air gap when the MOSFET is ON. It then transfers the stored energy to the secondary side and the load during the switch-off phase when the MOSFET is OFF. The turns ratio of the transformer determines the output voltage levels [16]. This converter topology is used in low to medium power applications due to its relatively lower efficiency compared to other topologies, such as the forward or full-bridge converters. However, its simpler control and capability to provide multiple outputs with isolation make it ideal for applications such as battery chargers, auxiliary power supplies in electronic devices, and LED drivers.

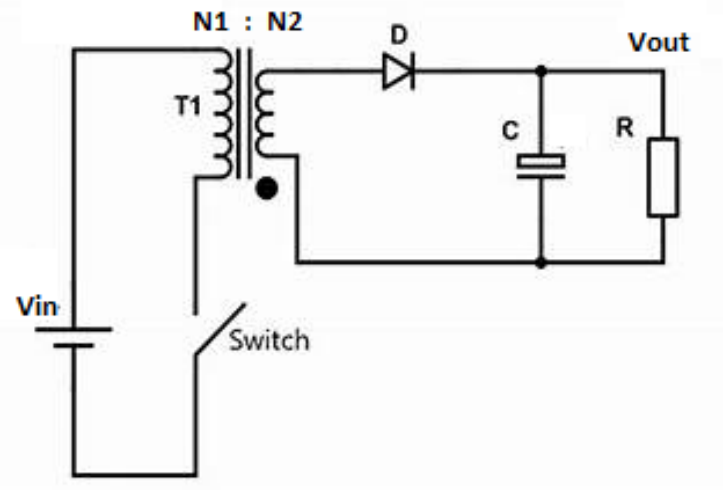

Figure 2.4: Flyback Converter Circuit Diagram

2.1.7 Forward Converter:

The forward converter is a type of non-isolated power converter that steps down a higher input voltage to a lower output voltage. During the on-state of the MOSFETs, the inductor is charged by the input voltage. When the transistor turns off, the inductor discharges to the load and completes the path through a freewheeling diode or synchronous rectifier. The converter consists of a switching element, inductor, diode, and capacitor for voltage filtering. This converter can operate in Continuous Conduction Mode (CCM), where a non-zero inductor current always flows during a complete cycle, or in Discontinuous Conduction Mode (DCM), The need for specifying electrical grounding between input and output requires using isolated DC-DC converters.

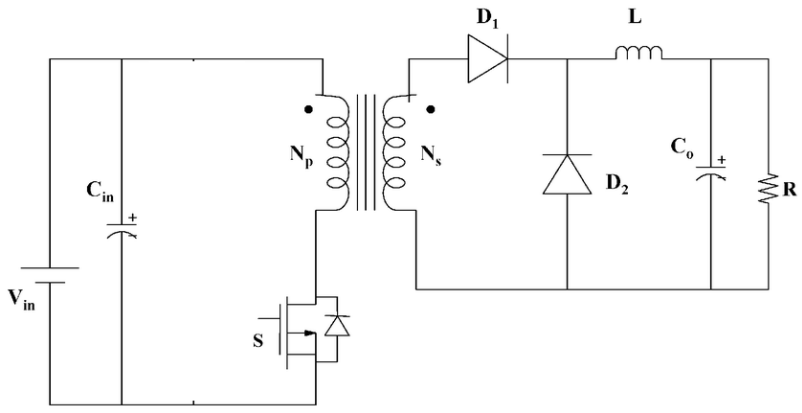

Figure 2.5: Forward Converter Circuit Diagram

2.1.8 Push-Pull Converter:

The push-pull converter employs a center-tapped transformer in conjunction with a half-bridge topology. In this configuration, the MOSFETs are driven in a complementary manner, ensuring that during each switching cycle, one half of the primary winding is energized. When MOSFET A when this device activates power flows in one portion of the primary winding to put energy in the transformer. transformer. The stored energy transfers during the switch-off period from the MOSFET A storage to the secondary side of the circuit. secondary side via the opposite half of the primary winding. Engineers use this topology because of its efficiency to implement medium-power applications. MOSFET A operates along with an automotive electronics system and telecommunications infrastructure. Its design contributes to steady input current, reduced noise on the input line, and enhanced performance in higher power scenarios. [17].

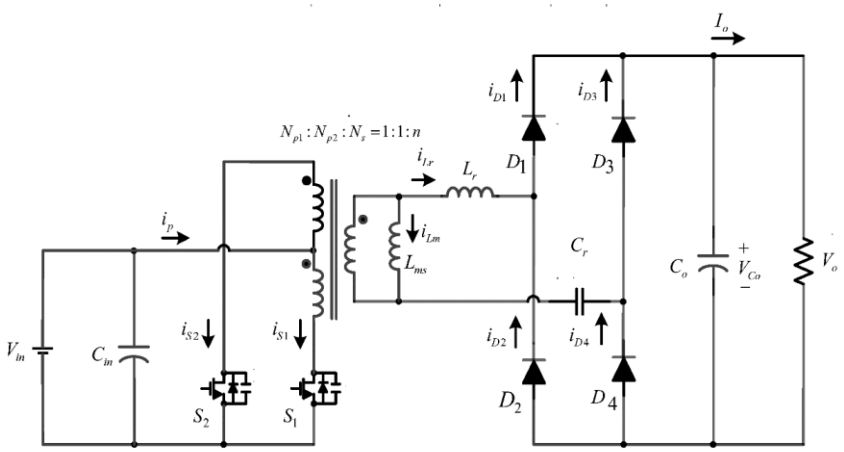

Figure 2.6: Push-Pull Circuit Diagram

2.1.9 Full-Bridge Converter:

A versatile power converter named full-bridge converter enables power delivery and regeneration functions. This converter allows bidirectional power transfer which enables applications that need power delivery as well as regeneration. It employs Four MOSFETs constructed as a bridge system work with a transformer to produce electrical functionality. isolation and voltage conversion. The system can produce control signals through pairs of complementary MOSFET operation. an alternating current (AC) voltage. The timing periods of these switches function as the basis to define the output voltage power level. The precise voltage regulation becomes possible through this arrangement that controls

the output voltage [18]. This arrangement provides high efficiency characteristics which makes it suitable for medium and high-power applications. The topology determines the function of the power system which aids data centers and electric vehicles.

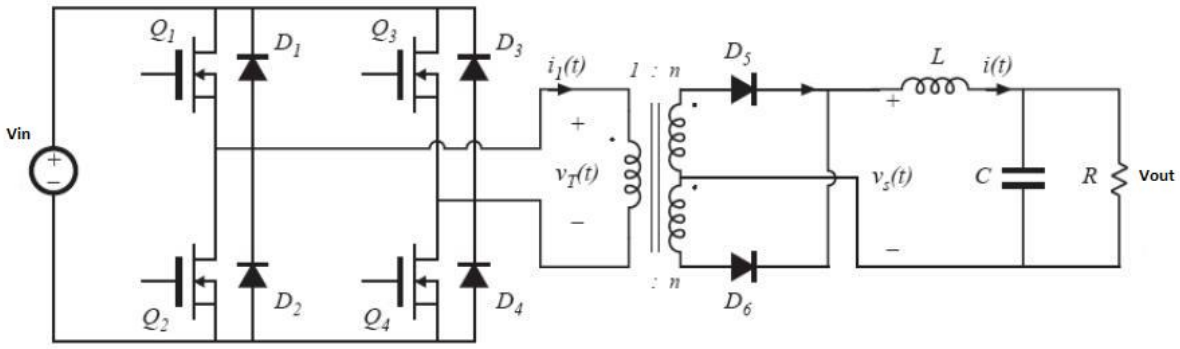

Figure 2.7: Full Bridge Circuit Diagram

2.2 Overview of Current Topologies Employed in EV Chargers:

The basic design of fly back converters enables easy implementation of control methods for both directions of operation. When transformer leakage inductance occurs, it generates hard switching conditions that cause secondary side diodes to face reverse recovery challenges. The circuit recycles transformer leakage energy successfully to decrease switch voltage stress and solve reverse recovery issues [19].

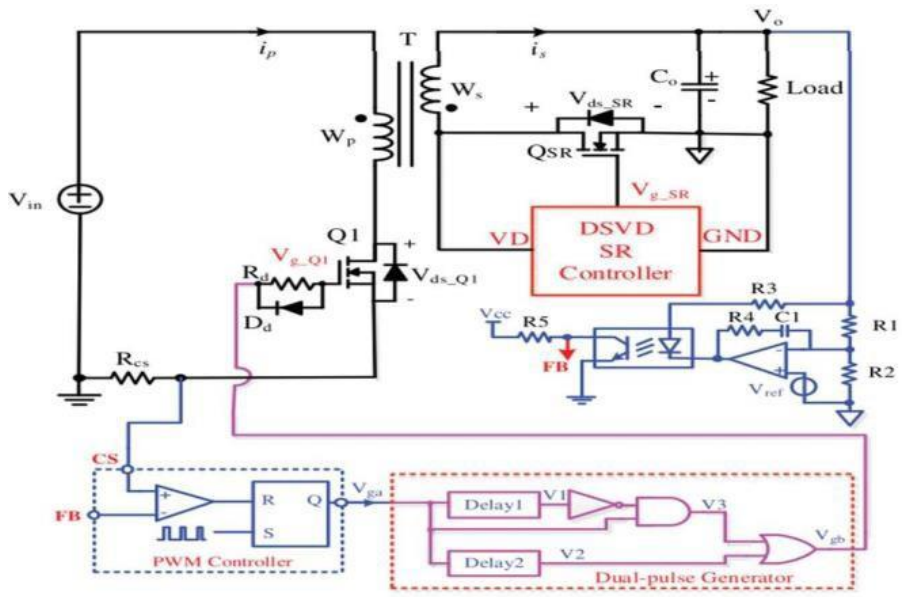

Figure 2.8: Fly back converter with SR Controller

Active-clamp circuits serve double functions by storing energy during primary side switch openings while allowing switches to close at minimal voltage levels due to which lower resistant switch elements can be used to boost overall efficiency rates. The energy saved inside the coupled inductor allows the primary side switch to perform ZVS (Zero Voltage Switching) during the turn-on transition. Turning these converters into Discontinuous Conduction Mode operation causes the disappearance of soft-switching attributes while escalating turn-off losses [20].

High turn-off losses can be reduced through converter operation under Boundary Conduction Mode (BCM).

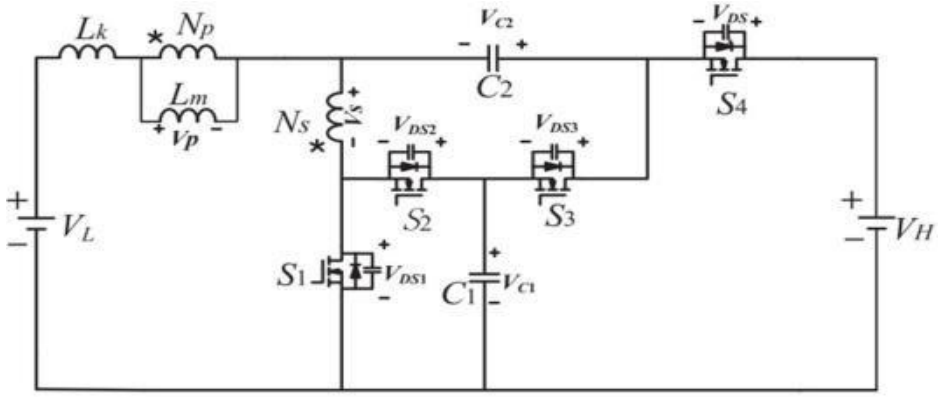

Figure 2.9: Non-Isolated converter with step up boost cell

Achieving stable and efficient operation across a wide output voltage range presents challenges in the design of magnetic components and filters. An alternative approach involves utilizing a two inductor-capacitor-diode snubber circuit, which absorbs the energy from the leakage inductance during turn-off events.

Despite the advantages of the single-ended fly back converter, the techniques discussed in the aforementioned sources may result in high voltage stress on switches and suboptimal transformer utilization. These limitations often necessitate the interleaving of multiple stages to meet high-power application requirements [21].

The wide-range converter proposed for electric vehicle (EV) applications in offers several advantages. It features an improved voltage gain transfer ratio while maintaining a common electrical ground, contributing to low-voltage stress on switches and overall high efficiency. The dead-beat controller operates in both DC-DC and unfolding stages of the converter. The implementation of dead- beat controllers supports accurate rapid system responses. Performance evaluations in bidirectional power Testing with V2G flow conditions supports the practical application of this converter. practicality. The

design implements efficient power transfer operations that link the vehicle system to the grid network. The innovative design plays a crucial role in improving every aspect of an EV's charging and discharging functions. The dead-beat controller enables rapid converter responses to all performing changes. The converter operates with stability throughout different load conditions. This power flow design integrates with current research on a system which allow vehicles to exchange power to grid. These vehicles establish a power connection to return electricity to the power grid for supporting electrical network stability while advancing sustainable energy practices. The successful integration of such a converter in EV applications. represents a significant advancement in the development of efficient and flexible charging systems power flow scenarios such as vehicle-to-grid (V2G) mode validate its practicality. Research by [22] presents an improved converter design with two key advantages based on better voltage gain transfer ratio and common electrical grounding functionality which leads to low-voltage switch operation and enhanced efficiency. The voltage transfer ratio of this converter stays synchronized with a common ground connection that leads to low-voltage stress on all switches and improves overall high efficiency.

The converter keeps a high-efficiency operation throughout a limited and specific range of voltages. The changes in voltage cause switching losses to increase while demanding better thermal management systems. The device faces challenges leading to potential long-term effects on reliability and operational performance stability across different operating conditions. operating conditions. Performance sustainability requires implementing solutions to these problems and robustness in real-world EV applications. The authors introduce high- frequency isolated bidirectional converters which depend on single-phase-shift and dual-phase-shift control methods. This demonstrates two control techniques including single-phase-shift control and dual-phase-shift control which enhance system receptivity in normal and reversal scenarios. reverse operation. Insufficient precise phase shift control introduces multiple difficulties that affect system performance. The efficiency decreases while electromagnetic susceptibility increases.

The converter presented in [23] obtains high voltage gain through two interconnected flyback transformers arranged in parallel. The input parallel connection of two flyback transformers reduces the required size of the capacitive filter. The converter achieves high voltage gain because of its output connection arrangement in series. However, the Operating the two flyback transformers simultaneously requires careful management due to their complex nature leading to operational instability and efficiency problems. efficient operation under varying load conditions. The converter described in [24]

demonstrates bidirectional functions for both V2G and G2V operations while providing elevated voltage gain characteristics through two flyback transformers implemented in parallel.

A step-up cell integrated into the circuit enables the achievement of high voltage gain. However, the converter has a common input and output ground. Without galvanic isolation between input and output sections high noise becomes an issue. The converter allows excessive current flow through vulnerabilities and shows high sensitivity to short circuits. Additionally, the A voltage gain instability exists in the converter design from [25] which features both a complex model structure and changes the voltage amplification considerably with trivial changes in its duty ratio. with minor variations in duty ratio.

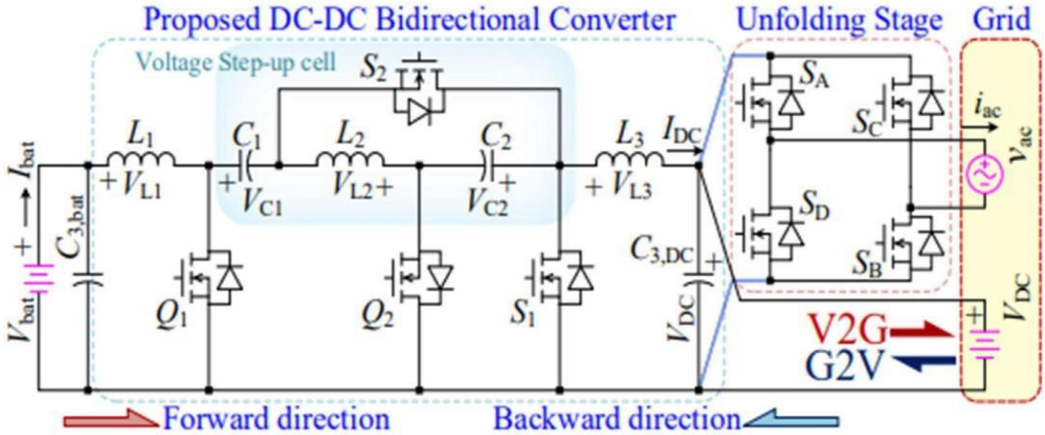

Figure 2.10: Bidirectional converter with Voltage step up cell for Enhanced High-Side Voltage Gain

The three-port bidirectional forward converter described in [26] features multiple advantages through its operation. The power sharing distribution occurs simultaneously with minimal energy storage because the system operates both primary and secondary sides simultaneously.

The selection of this design decreases magnetic component dimensions. The converter design requires several additional switches alongside its diode's components. The device introduces additional switches and diodes beyond standard forward converters which widens the duty cycle operational range. Some key advantages exist despite the operational restrictions of this converter. The converter has limited capability to reach Zero Current Switching mode. The output diodes obtain zero-current switching (ZCS) because of leakage inductance found in the transformer. Additionally, the design topology from [27] produces elevated switch voltages which leads to the need for selecting devices with higher breakdown voltages and drainage-source resistance to reduce power losses during the turn-on procedure. more expensive devices with higher breakdown voltages, higher drain-to-source voltages, and low the converter needs drain-to-source resistance with low values to reduce power loss

when the switches turn on. The BDC presented in [28] delivers high voltage amplification yet includes two LC filters for its design. The device incorporates LC filters at both the low-voltage zone and high-voltage zone to support continuous current supply. This design Raising power density is a fundamental requirement for these systems thus BDC's design choice leads to system growth and power density reduction. Onboard battery chargers (OBCs) need high power density as their main requirement. Additionally, the cascaded the cascade design of the converter system requires extra stress on the switches that must use more robust components. robust and potentially more expensive components.

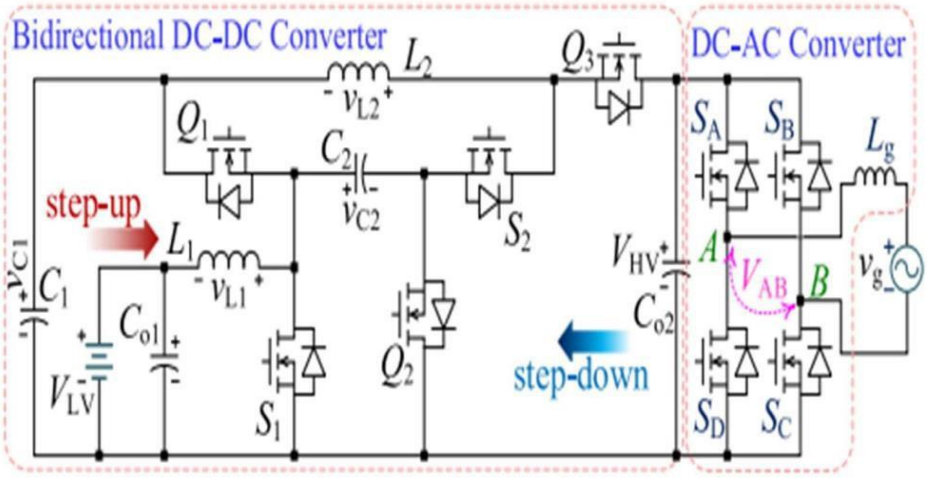

Figure 2.11: Bidirectional converter with High Voltage gain and DC-AC unfolding stage.

The A dual active bridge (DAB) converter serves as the central element in electric vehicle (EV) power electronics because it facilitates bidirectional power flow and maintains high operational efficiency. The converter features electronics power that operates in reverse and delivers efficient performance. Advanced control strategies, efforts to accomplish full load range zero voltage switching (ZVS) require particular attention. The implementation of this technology leads to minimized switching losses together with better efficiency performance. Implementing an optimized The Extended Phase Shift control methodology allows converters to perform fluid transitions. The control system performs ZVS switching operations across different load ranges without exceptions. Researchers acknowledge the limitations of obtaining soft switching within predefined voltage ranges as one of the challenges with this solution. The system presents drawbacks that must be considered in detail before deploying such systems at practical scales. To Academic professionals have proposed different strategies to handle these difficulties. For instance, an artificial-intelligence-based hybrid EPS modulation for the DAB converter is described in [29]. The researcher strives to maximize ZVS operation range and efficiency

through the converter's design. The new technology seeks to enhance power density by lowering the stress on components for suitable use in electric vehicle onboard battery charger systems. Such technology works best when applied to onboard battery chargers for electric vehicles.

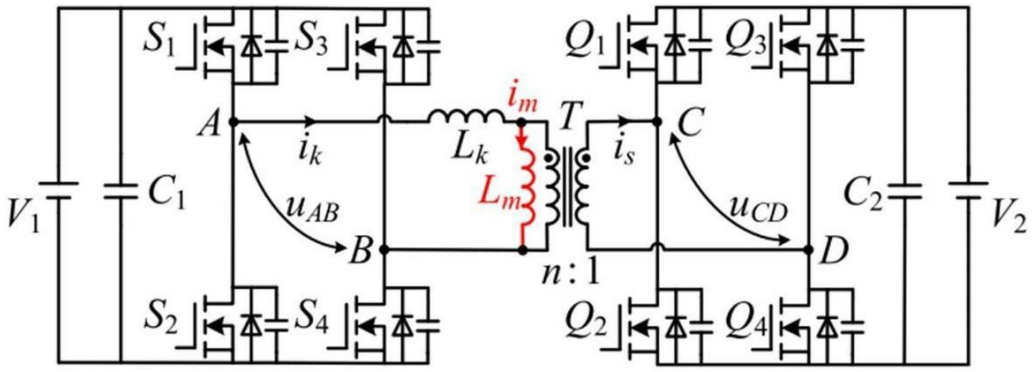

Figure 2.12: Dual Active Bridge Converter with EPS control

The high step-up resonant converter presented in [30] includes active-clamping on its primary side and a T-type structure on its secondary side to achieve high step-up gain and minimize switching losses in active switches. The dual structure of a T-type configuration on the secondary side combines with primary side active-clamping to produce an efficient and cost-effective design. The proposed high step-up resonant converter operates with high voltage transformation and low loss on active switch components. However, the converter system does not provide two-way functionality that would support application needs for onboard battery charging systems in electric vehicles specifically battery chargers (OBCs). The converter operates bidirectionally after its output diodes get replaced with switches during application of conventional switching modulation. The inability to apply conventional switching modulation occurs because the single diode rectification in the primary side creates power transfer disruptions. power transfer. The converter cannot obtain necessary operational conditions because of this restriction. backward power flow. The implementation of boost switches causes excessive stress to interfere with power consumption within power MOSFETs. The voltage ratings of selected switches need to be increased for proper operation. This requirement increases the high cost of the converter represents a disadvantage that renders this device inappropriate for uses requiring maximum cost effectiveness. The issue requires solutions which alternative converter topologies with bidirectional capability have been developed to resolve them. been proposed. For instance, the high

step-up high step-down bidirectional DC/DC converter discussed in [31] offers bidirectional power flow with improved efficiency and reduced component stress.

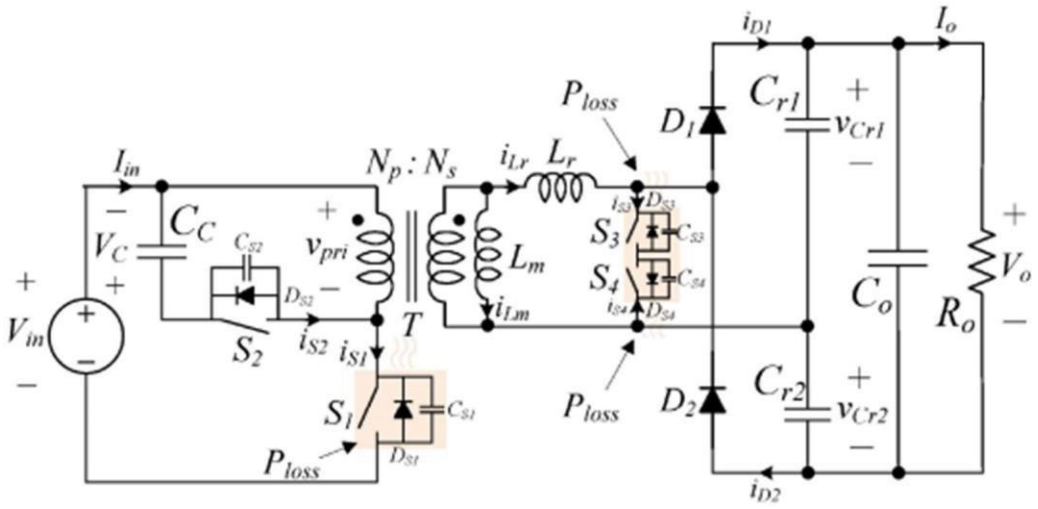

Figure 2.13: Isolated Bidirectional Resonant converter with Active clamped primary and T-type voltage Doubler circuitry

The resonant DC–DC converter with bidirectional capability presented in [32] provides a solution for applications requiring bidirectional power transfer. To address the limitations of single-ended configurations in bidirectional power transfer, an alternative approach introduces an active-clamped push-pull circuit on the primary side. The design incorporates two rectifier diodes as active clamps that enable power flow through active clamp circuits during both first and subsequent half switching periods. The design includes two rectifier diodes which enable power flow through distinct paths both in the beginning and following switch period halves. As a result, backward power. The method accomplishes transfer operations which maintain operational characteristics in forward missions. However, this solution necessitates the inclusion of two additional switches and an extra winding on the primary end of the transformer. The insertion of additional components enables extended bidirectional operations for the converter at the cost of larger size and higher expenses. The converter dimensions alongside its cost increase due to these components may limit its practical use. The converter should be evaluated for applications that require both limited space and restricted budgets. For instance, in onboard battery chargers (OBCs) for electric vehicles (EVs), where high power When high power density along with low costs matter the elevated number of components combined with their higher expenses.

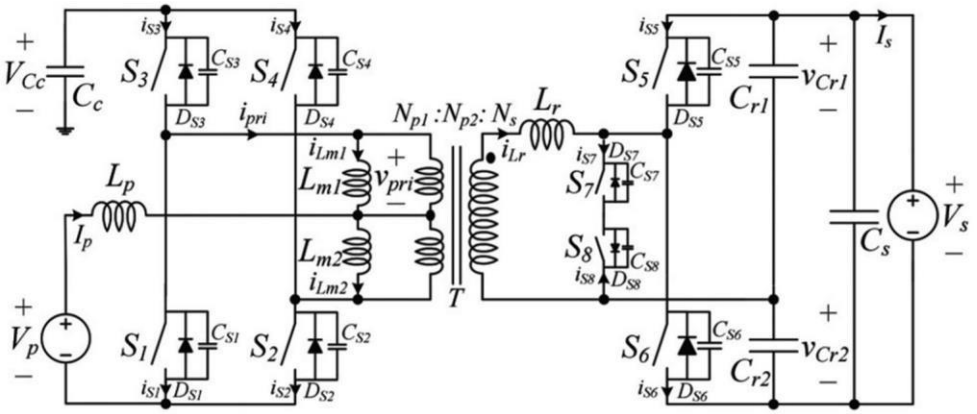

Figure 2.14: Push Pull DC-DC Converter with T-type voltage doubler

suitability. The implementation of such a converter will encounter various operational difficulties. Therefore, while the active-clamped push-pull circuit the design provides enhanced power interchange capabilities while requiring attention to the effects on dimensional aspects as well as cost elements. The evaluation process requires assessing complexity as an essential factor for particular applications. A duty compensation enhancement has been implemented in the bidirectional DC-DC converter described in [33]. control mechanism. The forward operation of this converter is built with a push-pull resonant boost topology. transformer, enhancing efficiency and performance. The converter works as an in reverse direction operation. Within the neutral point clamped (NPC) configuration the device operates as a resonant mode converter to transfer power effectively. transfer in both directions. Such design methodology provides an effective solution to manage bidirectional power issues. The system provides a flexible solution because it completes efficient energy conversion tasks in multiple operational directions. directions.

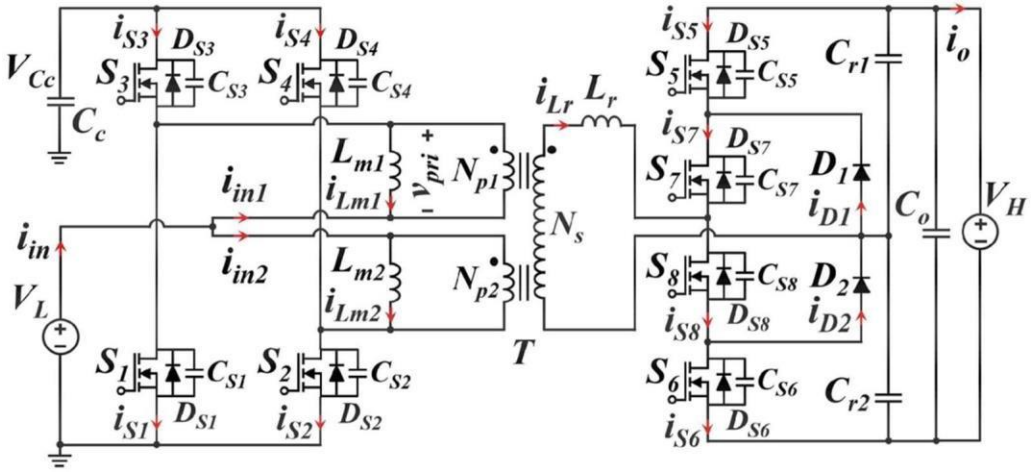

Figure 2.15: Push Pull DC-DC Converter that contains an NPC Type secondary side arrangement.

In The design technique successfully handles problems present in dual-direction power operations. The system fulfills diverse energy conversion needs because it handles power flow efficiently between forward and reverse directions. The placement of four switches serves as an effective method to reduce input current ripples in push-pull converter systems. ripple, enhancing performance. The configuration diminishes power density because of its implementation. to the additional components, such as two bulky transformers and four switches. Not all the input ripple demands from applications vary from low to high since electric vehicle charging systems need minimal ripple but certain applications do not. The conversion process through onboard converters uses moderate current ripple levels in their operations. The combination of high-power density and low cost with retention of substantial efficiency can be achieved through different converter topologies. converter topologies are considered. Micro-mobility applications benefit best from these converter designs [34]. The design space for electric bikes and motorcycles requires such technology because they face tight dimensions and high-cost requirements. By When components are optimized through design the result becomes a balanced outcome between performance and practical aspects. requirements of these applications. The research into power topology designs for EV charging stations focuses mainly on importance of energy density and system efficiency.

The study observes that raising power-generation levels through increased power without enlarging converter sizes demonstrates improved operational performance along with cost efficiencies. The cost effectiveness and operational improvement come from expanding the converter dimensions alone.

2.2.1 Comparative Study of Different Power Stage Topologies:

A major limitation of this configuration exists due to its excessive number of switches that raises operational complexity and associated expenses. More transformers used in a system increases both implementations expense and reduces power capacity density. efficiency and compactness in practical applications. The excessive use of turns in devices has negative effects on parasitic responses. Voltage spikes along with noise levels become problems because they generate electromagnetic interference (EMI). concerns [35], [36]. Furthermore, the need for complex control strategies and limitations on soft A severe limitation exists because of restricted operational ranges and soft switching restrictions [37]. Realizing solutions to current power converter challenges will lead to improved power converter efficiency together with reliability and scalability potential. converters for various industrial applications.

2.3 Feedback Control Techniques used in DC-DC Converters

In The following segment presents an in-depth analysis of feedback control approaches which operate on DC converters. DC converters. Control feedback systems play an essential role to preserve both the operational stability and performance quality along with the power efficiency of Electric vehicle (EV) charging requires efficient use of power converters in their dynamic operation. The selection of A control method directly shapes the performance of transient response and output voltage ripple together with overall converter efficiency. voltage ripple, and overall efficiency.

2.3.1 PID Controller

A P-I-D controller functions as a popular feedback regulatory system for industrial process monitoring. The controller enables professionals to maintain control of process variables including temperature pressure flow and position. PID stands for the controller operates through three computational terms known as PID that describe its output generation process output [38]. The proportional term produces output that directly relates to the difference between the desired setpoint and actual process value. and the current process variable. The I term minimizes all errors throughout a specific timeline to produce output signals the generated output through the PID controller depends on the total error collection. The output driven by the derivative term is proportional to error variation rate. The controller output grows directly with the speed of error changes. A PID controller obtains its responsiveness through the combination of adjustable coefficients which integrates these three control variables. The PID controller detects various system errors and disturbances including steady-state errors together with oscillations and overshoots. The PID controller works by measuring the process variable then checks it against the desired set point in a continuous cycle. The system uses feedback control to manage its output based on error measurement for maintaining stable and precise operational control.

The output of a PID controller is typically calculated as follows:

$$Output = K_p \times e + K_i \times \int e(t)dt + K_d \times \frac{d_e}{dt} \quad (1)$$

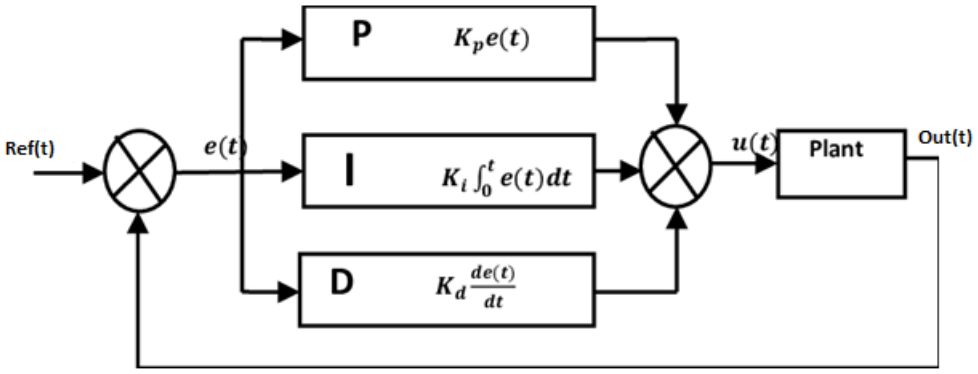

Figure 2.16: Feedback control implementation using PID

K_p is the proportional gain serves as the constant parameter which controls the strength of the proportional element.

K_i represents the integral gain which sets the strength of the integral section of the controller

K_d controls the force of the derivative term in the control system.

The error signal 'e' indicates the change which develops from the setpoint difference and process variable measurement. The time integration of error signal e(t) yields the resulting value ∫e(t) tithe time derivative of the signal determines de/tithe terms in the mathematical expression describe P control along with I control and D control. An adjusting process selects these gain values to fulfill required system performance specifications regarding stability speed and accuracy. The implementation of PID control methods enables stable converter operation by controlling the output parameters. The PID controller generates an error signal by computing the difference between required output and system output before applying P, I and D terms to adjust converter D. The proportional output of the controller matches the system error against the required output while the integral section integrates time-based error to minimize steady-state errors and the derivative part works with error variations to stop oscillations and overshoot. The practical implementation of PID controller requires tuning the controller gains to achieve steady system stability while managing speed response and minimizing performance issues like overshoot and ringing and instability [39]. The efficiency of DC-DC converters improves when PID control works simultaneously with feedforward control or adaptive control in various operating conditions and applications.

2.3.2 PID Control utilization in DC-DC Converter

DC-DC converters rely on PID as an integral component for managing stability as well as regulation and ripple performance. The output signal from the DC-DC converter flows to an error amplifier before entering the PID Controller together with Vref. The PID controller creates the appropriate duty cycle settings for a DC-DC converter system [40]. The PID system modifies its duty cycle in response to detected output changes as shown in Figure 2.17.

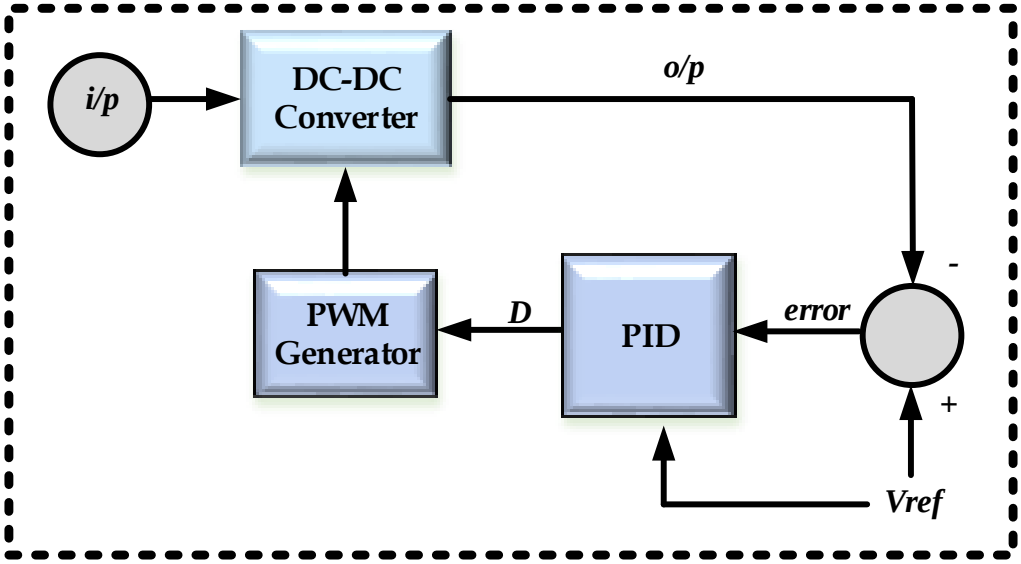

Figure 2.17: Feedback control of DC-DC using PIDs

2.3.3 Sliding Mode Control

The control of DC-DC converters receives management through the implementation of sliding mode control (SMC) integrated with electronic circuits to transform DC input voltage into distinct DC output voltage levels. DC-DC converters find extensive application throughout power electronics systems as they connect with different power supply and renewable energy projects and electric vehicle infrastructures [41]. The main objective in DC-DC converter control is to stabilize output voltage performance despite variations in input voltage along with changes in load conditions and other interfering disturbances. Through SMC design practitioners can develop a stable control method that maintains converter stability at the required output voltage across different disturbances. When designing an SMC controller for DC-DC converter control the initialization process begins with the creation of a specific sliding surface that divides appropriate and inappropriate system actions. The

converter output voltage error together with its derivative forms the basis for describing the sliding surface. A control law is established to send the system directionally toward the specified sliding surface while maintaining constant surface travel. A control signal made of continuous elements and discontinuous switching components ensures system stability on the sliding surface. The performance evaluation of SMC controller requires both simulation tests and physical laboratory experiments. The implementation of SMC produces outcomes with strong disturbance rejection as well as swift response characteristics and strong protection attributes. The process of designing sliding surfaces together with parameter tuning demands specialized expertise because it poses multiple difficulties.

2.3.4 Model Predictive Control

Through model predictive control (MPC) the control technique creates best control actions by generating forecasts of future system behavior based on system models. DC-DC converters attain output voltage regulation through predictive control systems that minimize cost function values by producing appropriate control signals according to MPC methodology [42] To implement MPC for DC-DC converter control systems must have appropriate mathematical description available. The model design dependent on converter topology selection between linear and nonlinear architecture as well as precision needs. The model requires both converter dynamics with inductor current and capacitor voltage components along with the converter switching devices. After acquiring the available model developers can create an MPC algorithm. Modeling future voltage output of converters enables the generation of new signals that aim to minimize designated cost functions. The cost function uses performance criteria that involve settling time and overshoot together with energy consumption. [43] The disturbance rejection performance of MPC is superior and it maintains control over input and output constraints while operating. DC-DC converters receive an effective solution through MPC controls to accomplish high precision and application-critical reliable operation. The way a cost function is designed and control parameters get tuned determines how well the MPC controller performs.

2.3.5 ANN Based Control

The acronym ANN signifies Artificial Neural Network derived from human brain neural network structures. Each input carries significance weight before a non-linear activation function transforms the output of each neuron. At the training stage system adjusts the weights and biases of its neurons through learning algorithms that reduce output prediction errors matched against required training data outputs. The training aims to establish a performable function that generalizes unobserved testing data and predicts accurate results or classifies correct classifications.

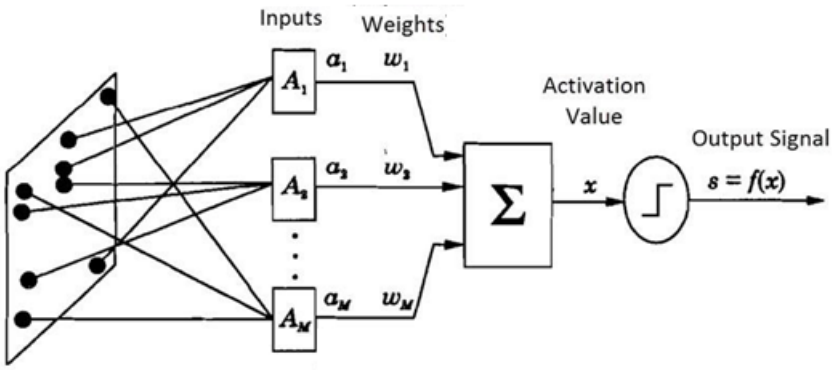

Figure 2.18: Feedback Control of DC-DC using ANN

2.3.5.1 Comparison of ANN with SVM and Fuzzy Logic

Recently, application of ANN based control has shown advantages over other machine learning techniques like SVMs and FLC for the control of DC-DC converters in terms of computational efficiency, real time performance and implementation trade off.

SVMs have a slower convergence characteristic in the process of training compared to ANNs. The case specifically is that ANNs require up to 36~42% fewer training iterations compared to SVMs in achieving the same voltage regulation accuracy in the DC-DC converters [44]. The reason behind this reduction is that ANNs are inherently parallelizable, allowing the training data to be run in parallel while SVMs need to solve a quadratic optimization problem, which is sequential. In addition, unlike support vector machine, ANNs do not need to retrain from scratch for each new operating condition in real time.

In terms of real-time performance, ANNs outperform fuzzy logic controllers. Studies have shown that ANNs process transient event significantly faster by an average of 4.7µs as opposed to 8.2µs for fuzzy logic systems [46]. The reason for this performance difference is that ANNs carry out direct input-output mapping, a principle that bypasses rule base evaluation costly to many fuzzy systems. Finally, more effectively handling the dynamic changes in load and the fact that fuzzy logic has to be recalculated as soon as there is a change in conditions makes it easier for ANNs to cope with changing system conditions and quickly adapt and learn from changing conditions.

In terms of memory usage and computational cost the ANN fits between the classical methods such as PID and more complex methods as fuzzy logic. For example, ANNs use 4× less memory than equivalent fuzzy logic controllers which have typically large rule bases that are used to operate (Texas Instruments [47]). As embedded systems with limited amounts of memory resources have smaller problem sets, this makes ANNs more suitable for such systems. Compared to PID control, ANNs have 2.1× more memory

requirement, but they do not require manual tuning of parameters for each operating point, and this is an extremely important improvement in dynamic environments.

2.3.5.2 Advantages of Feedforward Neural Networks (FFNN) for Control

Feedforward Neural Networks (FFNNs) has several advantages over more complex architectures such as Recurrent Neural Networks (RNNs) or Convolutional Neural Networks (CNNs) were used to select the type of ANN, because of their low computational complexity, a fast training speed and real time inference. RNNs and a CNN are relatively more complex structures than FFNNs, and hence have a higher computational complexity. RNNs behave recurrently in terms of information processing and hence they have to store and process information from previous (previously) time steps, which come with a high overhead of computation. However, CNNs are powerful for spatial data processing tasks and require more computational power to extract features, which is less required in control systems of power electronics [48].

FFNNs are good for real time applications as they have a faster inference as the input data is processed in a feed forward manner. The distinction to RNNs, which demand processing in the sequential manner, and the CNNs, which require convolutional layers for greater processing time, is that FFNNs can perform fast computation through only one pass in the network [48]. It shows that the system can respond to load changes and in other dynamic conditions.

By having no time dependent or spatial dependent components, FFNNs require less additional computational resources and are much quicker to train than RNNs and CNNs. More complex architectures (e.g., in RNNs or in CNNs) as well as an association with processing sequential data (RNNs) or in a convolutional manner (e.g., CNNs) require greater amounts of training time for RNNs and CNNs respectively. Conversely, FFNNs directly map inputs to outputs that yields faster convergence during training, and thus are useful for real time control application [49].

2.4 Replacement of PID with ANN

Some research studies established that Artificial Neural Networks can replace traditional Proportional-Integral-Derivative (PID) control methods in DC-DC converters. A n ANN-based control system learns control actions through a data-driven training process for system states instead of using manual parameter adjustment like PID controllers do. The neural network system can adapt effectively to nonlinear and complex system behavioral patterns which makes it highly effective for scenarios where conventional control approaches fail to achieve optimal performance [50].

During operation the present state of the system gets fed into the neural network which generates an output to determine the control action through the DC-DC converter duty cycle. The training stage of ANN involves weight and bias adjustment to minimize differences between forecasted results and system measurements according to Figure 2.19 This process enables the ANN to learn the underlying relationships between system inputs and outputs, allowing it to generate control actions that optimize system performance [36].

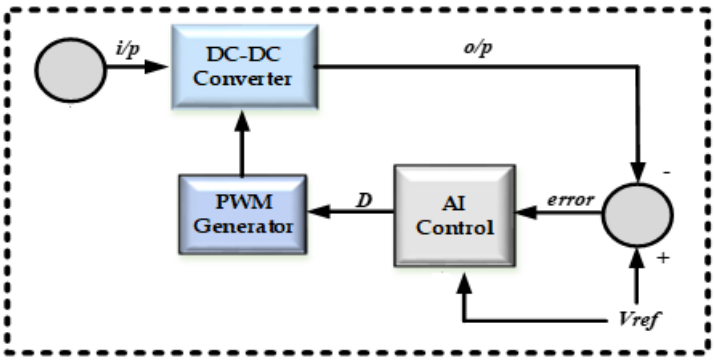

Figure 2.19: Implementation of Feedback control of DC-DC using ANN

After the ANN is trained, it becomes operational; it accepts real-time system inputs and issues control actions that adjust to changes in the system. One of the significant advantages of ANN based controllers is its ability to adapt. ANN based controllers can better handle process nonlinearities and dynamic operating conditions compared with traditional PID controller. Such is the case for ANN-based controllers applied, for example, to DC-DC converters where they are shown to improve system response to transient operations, decrease the output voltage ripple, and further enhance system stability under variable load conditions [51].

ANN based controllers are one of the most significant advantages because they can deal with nonlinear

system. The DC to DC converter often has nonlinear behavior caused by its switching dynamics, parasitics etc. Traditional linear PID controllers base on linear control theory do not have sufficient flexibility to provide the best performance in such scenarios [52]. On the other hand, ANN controllers can optimize and adjust to the nonlinear performance of the system, however stable and effective operation under disturbances can be maintained.

ANN based controllers are generally very flexible to a dynamic operating condition and are nicely suited for applications such as renewable energy systems and electric cars. The DC-DC converters operate under rapidly changing uncontrolled operating conditions in these applications. Currently, ANN based controllers can optimally perform under all conditions and can adapt online to all changes. Achieving this adaptability is through using online learning techniques where the ANN parameters are updated in real time as a function of the system's current state. [53]

CHAPTER 3: METHODOLOGY

The research presents a high-density DC-DC converter design. The converter implements active clamping on its primary side and operates with a secondary side that uses neutral point clamping (NPC). The converter reaches high power density because its actively clamped primary design reduces the number of components required. This compact design is the system reaches maximum efficiency through dynamic management of switching patterns utilizing AI-based algorithms switching patterns and improve ripple, system stability to non-linearities and load disturbances. The proposed novel modulation method enhances the converter to manage power flow. Under unbalanced DC offset currents the actively clamped primary side maintains its power flow capabilities. Unlike In contrast to fixed control variables used in traditional PID control the suggested AI-based control system operates adapts to varying operating conditions. The forward operational mode allows the duty ratio manipulation of the two central switches between primary and secondary devices. AI algorithms dynamically adjust the voltage gain through modifications to the secondary side elements. The AI controller helps the system to operate with intelligence to manage the sequence of primary and secondary side switch operations. A system control manages the switches through their operation for achieving efficient power transmission while minimizing losses and make it robust for varying load conditions. The power density and cost efficiency improve because AI-based modulation controls offer superior performance. The actively clamped primary side installation enables power transmission while boosting system power density and lowering system cost. The system achieves better power density. The AI controller operates to find the ideal switching sequence which achieves maximum performance and reduce the need for additional hardware components. The converter features a combination of a series resonant tank along with an NPC structure to achieve high efficiency and soft switching operation. Soft switching functions (ZVS) and high efficiency can be reached through this design implementation. The AI control system enhances this by predicting and optimizing switching transitions, further reducing switching losses and improving overall efficiency.

Comprehensive Analysis and Validation: A detailed mathematical analysis is presented, supported by theoretical operating waveforms and current paths for both forward and backward modes. The AI control system is rigorously tested and validated through simulations and capable of handling 1 kW

power with an input range of 50V to 70V on the low-voltage (LV) side and a regulated high-voltage (HV) side of 380V.

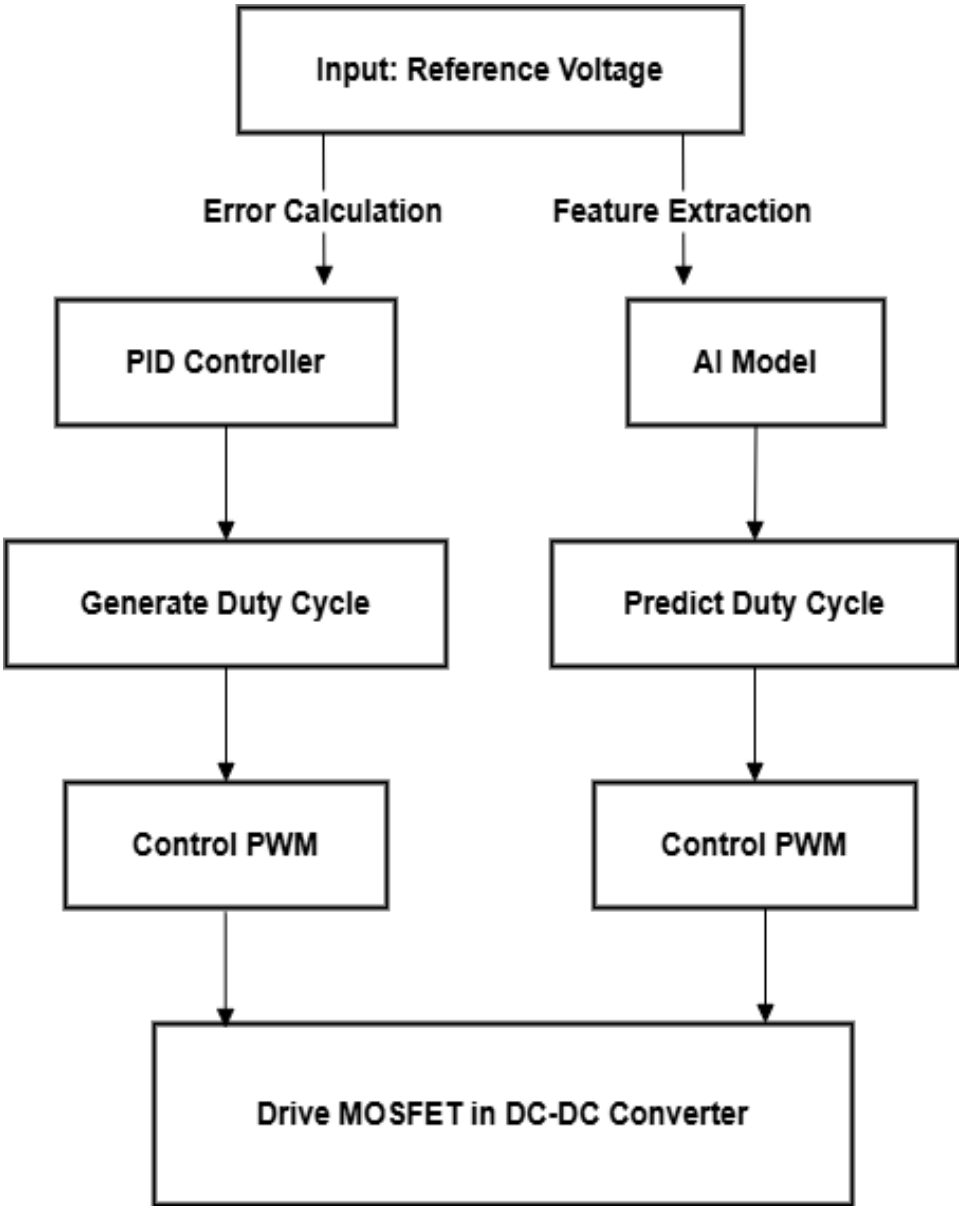

Figure 3.1: Comparison of PID & ANN

3.1 Theoretical Evaluation of Circuit Topology

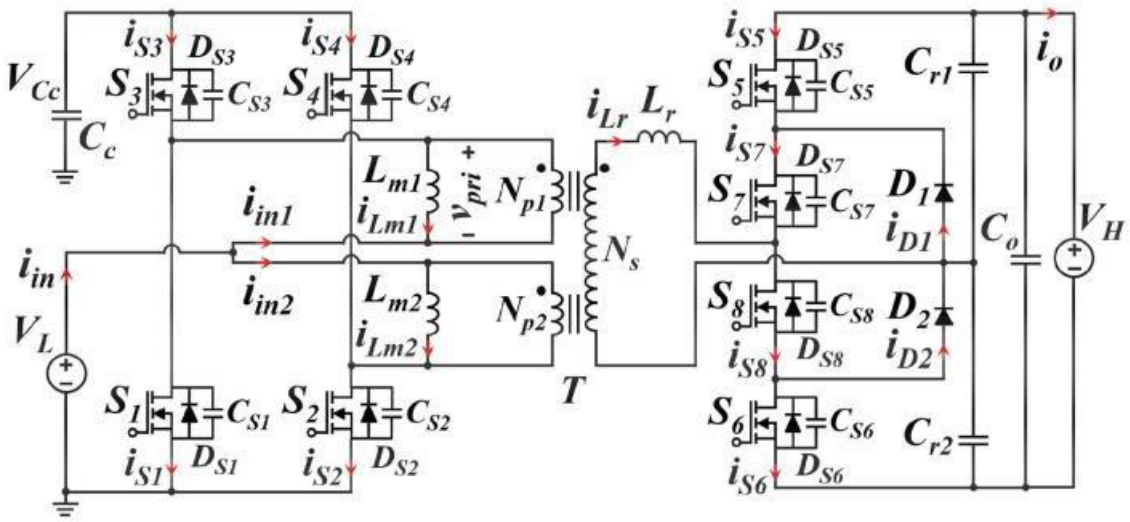

Figure 3.2: Resonant Actively clamped NPC-Type DC-DC Converter

Figure 3.2 shows the bidirectional actively clamped NPC type resonant DC-DC converter. The conventional Neutral Point Clamped (NPC) structure with a Push-Pull type primary side, as proposed in [54], achieves low current ripple but at the expense of reduced power density. This is due to the use of more components in control stage and also feedback loop is unable to remain stable for sudden varying load conditions and produce a ripple at output. To address this limitation and improve power density while reducing the number of switches, the proposed topology introduces an AI based control technique to mitigate the said issues.

In the conventional T-type structure with an actively clamped primary side, as presented in [55], the converter is limited to forward operation because it lacks single diode rectification on the primary side. Consequently, the topology and modulation scheme in [56] cannot support reverse power flow. To overcome this issue, current-fed PWM Push-Pull resonant primary side structures were proposed in [17] and [57]. However, these solutions require two additional switches and an extra transformer, leading to increased costs and lower power density.

To achieve higher power density, the proposed converter, illustrated in Figure 3.2, features a core switch S1 and a complementary switch S2 with a clamp capacitor Cc in series on the primary side of the transformer. The secondary side of the transformer T employs an NPC structure, where S_k represents the

switch designator, CD_{sk} denotes the drain-to-source capacitance, and D_{sk} is the body diode (k = 0, …. 6). The transformer parameters include the magnetization inductance L_m and the turns ratio n= N_{sec}: N_{pri} where N_{pri} and N_{sec} are the number of turns on the primary and secondary sides, respectively. A resonant inductor L_{res} forms a series resonant tank with the resonant capacitor $C_r = C_{r1}$ + Cr2. The currents flowing through the switches are denoted as i_{swk}, while i_{Lres} represents the current through the resonant inductor. The output capacitor Co and the clamp capacitor Cc are chosen to have sufficiently large values to minimize output and input voltage ripple.

This design aims to achieve high power density, efficient operation, and reduced voltage ripple while addressing the limitations of previous topologies.

Modulation Scheme Description: In the forward direction, the switching sequence is same as described in [54] i-e the control variable for adjusting the voltage gain is the overlapping duty ratio of switches S_5 and S_6 on the secondary side of the transformer. Meanwhile, the diagonal pairs of primary side switches are modulated with a fixed 50% duty cycle in a complementary manner. Throughout this operation, the topmost and bottommost switches of the secondary side NPC structure remain turned off. However, the body diodes of these switches facilitate a negative current flow at various intervals.

To address this limitation, a PWM signal with a fixed 50% duty cycle and a 180-degree phase difference is used to drive the switch pairs S_1 S_5 and S_2 S_6. Additionally, a separate PWM signal with a variable duty cycle is used to drive switches S_5 and S_6 in a complementary fashion, serving as the control variable for adjusting the voltage gain. By maintaining a fixed 50% duty cycle throughout the switching operation, unwanted DC offsets across the resonant capacitors $C_{r1}$and C_{r2} are avoided, ensuring balanced charging and discharging of these capacitors.

3.2 Forward Energy Transfer of the Converter (V2G)

In the forward mode, the operation of the converter can be divided into four distinct modes during the first half of the switching cycle T_0 to $T_{sw/2}$. These modes are illustrated in Figure 3.3, with the red lines indicating the current paths for each specific mode. Additionally, the state plane trajectory, which describes the combined linear and resonant operation of the converter, is depicted in Figure. 3.4 [54]. This trajectory provides a visual representation of the dynamic behavior of the system during the forward mode operation. The analysis of these modes and their corresponding waveforms and trajectories helps in understanding the converter's performance, including its efficiency, voltage gain, and resonant behavior, which are l for optimizing its design and operation.

Mode 1 [t_0-t_1]: When switch S_1 turns on, the magnetization current I_m begins to increase linearly, as illustrated in Figure 3.3. The voltage across the primary side of the transformer rises to V_L. The turn-on event of S1 achieves Zero Voltage Switching (ZVS), due to the negative current flowing through the body diode D_{S1} and the discharge of the drain-to-source capacitance C_{DS1} during the dead time t_{Df}. On the secondary side, switch S_6 remains on during this interval, causing the resonant inductor L_{res} to clamp diode D2, which begins to conduct. The voltage across the inductor during this mode can be described by the following equation:

$$L_r\left(\frac{di_{Lres}(t)}{dt}\right) = nV_{LV} \tag{2}$$

Rearranging (1) with initial condition being zero, inductor current value ($i_{Lres}(t)$) will be

$$i_{Lres}(t) = \frac{nV_{LV}}{L_r}(t - t_0) \tag{3}$$

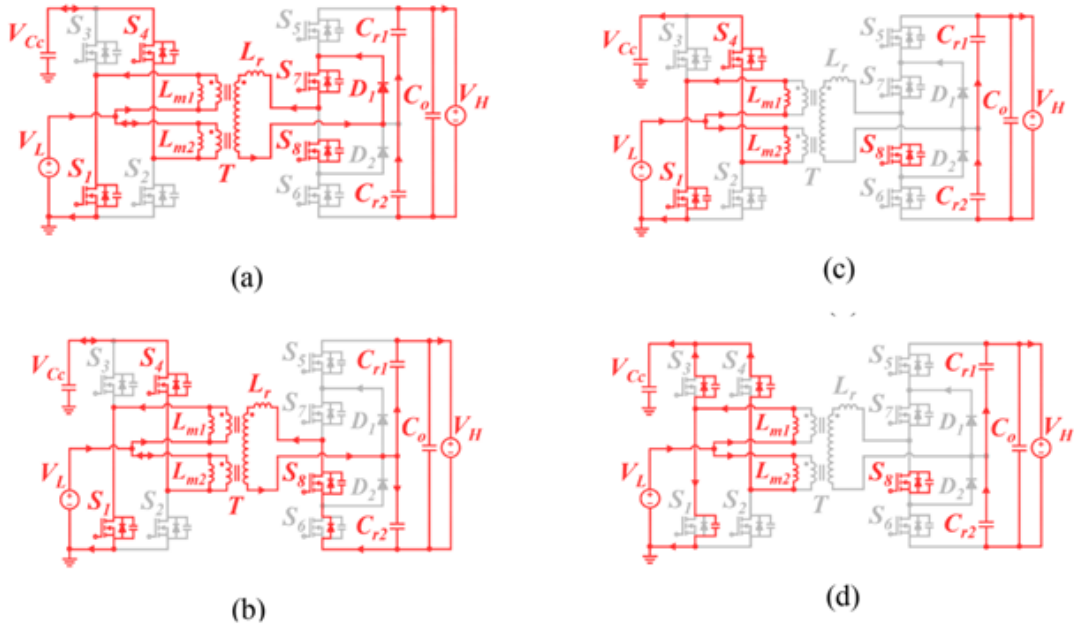

Figure 3.3: Equivalent Circuits of Neutral Point Converter (NPC) in various modes of Forward Operation (V2G)

The operating point moves from A to B along a line parallel to $Zri_{\text{Lres}}(t)$ from $[t0 \sim t1]$ as shown in Figure 3.4.

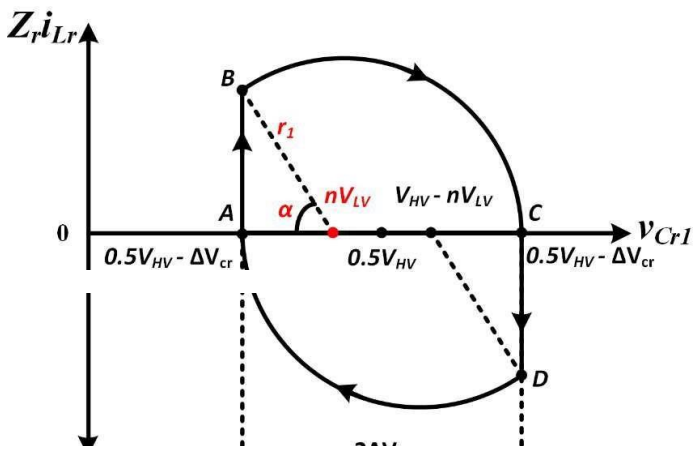

Figure 3.4: Forward Mode Operation: State Plan Trajectory of Converter

Mode 2 [t_1-t_2]: At time instant t1, switch S6 is turned off, which ends the linear operation of the resonant inductor Lres. The current now flows through the body diodes DS3 and DS5, causing the inductor to enter a resonant state. During this interval, a sinusoidal resonant current i_{Lres} begins to charge capacitor Cr1 and discharge capacitor Cr2. At time instant t2, the resonant current i_{Lres} drops to zero. The equivalent circuit and the current path for this mode are illustrated in Figure 3.5 and the voltage across the resonant inductor is given by.

$$v_{Lr}(t) = L_r \frac{di_{Lres}(t)}{dt} = nV_{LV} - v_{Cr_1}(t) \tag{4}$$

The current through resonant inductor is as follows.

$$i_{Lres}(t) = Cr_1 \frac{dv_{Cr_1}(t)}{dt} - Cr_2 \frac{dv_{Cr_2}(t)}{dt} \tag{5}$$

Since, $\frac{dV_{Cr_2}(t)}{dt} < 0$ and $Cr_1 = Cr_2$ thus,

$$i_{Lres}(t) = 2Cr_1 \frac{dv_{Cr_1}(t)}{dt} \tag{6}$$

The initial conditions at time instant t_1 for i_{Lr} and v_{Cr_1} are.

$$i_{Lres}(t_1) = \frac{r_1}{z_r} \sin(\alpha) \tag{7}$$

$$v_{Cr_1}(t_1) = nV_{LV} - r_1 \cos(\alpha) \tag{8}$$

Solving i_{Lres} and then rearranging yields.

$$i_{Lres}(t) = \frac{r_1}{z_r}\sin(\omega_r(t-t_1)+\alpha) \quad (9)$$

$$v_{Cr1}(t) = r_1\cos(\omega_r(t-t_1)+\alpha) + nV_{LV} \quad (10)$$

given by $\alpha = \sin^{-1}\left(\frac{nV_{LV}\omega_r}{r_1}(t-t_0)\right)$. The state-plane trajectory is shifted on v_{Cr_1} axis by nV_{LV} and the radius of the circular trajectory is $r_1 = \frac{V_{HV}}{2} + \Delta V_{Cr} - nV_{LV}$. The resonance frequency is $\omega_r = \frac{1}{\sqrt{LresCr}}$. and characteristic impedance of the resonant tank is $z_r = \sqrt{\frac{Lres}{Cr}}$. During this time duration, the operating point on state-plane trajectory moves from B to C as shown in Figure. 3.4.

Mode 3 [t_2-t_3]: At time instant t_2, i_{Lres} falls to zero and v_{Cr_1} is maximum i-e

$$v_{Cr1}(t_2) = \frac{V_{HV}}{2} + \Delta V_{Cr} \quad (11)$$

At time instant t3, the body diodes DS3 and DS5 experience a soft turn-off, achieving Zero Current Switching (ZCS), as no resonant current flows through the inductor at this point. Simultaneously, switch S2 undergoes Zero Voltage Switching (ZVS) turn-on. During this time interval, the operating point in the state plane trajectory remains at the same position as in Mode 2, i.e., Point C. This indicates that the system maintains its resonant state without significant changes in voltage or current dynamics during this transition.

The ZCS turn-off of the body diodes and the ZVS turn-on of S2 ensure minimal switching losses and efficient operation, contributing to the overall performance and reliability of the converter. During this operational mode the state plane trajectory stays at Point C which indicates the system maintains stability.

Mode 4 [t_3-t_4]:

The controller follows Mode 4 [t3-t4] by flipping S_1 off at time t_3 while enabling S2 switching with Zero Voltage Switching (ZVS) at time t_4. ZVS turns on the system because the drain-to-source capacitance C_{DS} of S_2 completes its discharge as noted through Figure 3.4. During this time interval, the operating point in the state plane trajectory remains at Point C, indicating that the system's resonant state and energy dynamics remain unchanged. This transition ensures efficient switching with minimal

losses.

3.3 Duty Cycle Impact on Forward Voltage Gain

The volt second balance $< V_L >$ for the primary side of the converter is should be zero in complete switching cycle and is given by.

$$< V_L > = 0 = nV_{LV}D_sT_{sw} - nV_C(1 - D_s)T_{sw} \quad (12)$$

Where D_s is the fixed duty ratio for primary side switches and is 50% of the switching period (T_{sw}) and V_{LV} is the low side voltage level. Therefore solving (12) yields

$$V_{LV} = V_C \quad (13)$$

Since the circular trajectory is centered at $(nV_{LV}, 0)$ in the forward mode, voltage across resonant capacitor $C_{r1}\ is\ v_{Cr_1}$ and the current i_{Lres} passing through resonant inductor is

$$i_{Lres}(t) = \sqrt{\frac{r_1^2 - \left(V_{Cr_1}(t) - nV_{LV}\right)^2}{Z_r^2}} \quad (14)$$

The time interval $[t_0 \sim t_1]$. is the time for which the main primary switch S_1 conducts thus,

$$i_{Lres}(t) = \frac{nV_{LV}}{L_r} D_F T_{sw} \quad (15)$$

$$V_{Cr1}(t) = \frac{V_{HV}}{2} - \Delta V_{Cr} \quad (16)$$

Where $t_0 < t < t_1$ and D_F is the Duty cycle for forward mode and ΔV_{Cr} is the change in voltage across resonant capacitor C_{r1}

Equating (15) and (16) in (14) results in

$$D_F = \frac{L_r}{Z_r n V_{LV} T_{sw}} \sqrt{2\Delta V_{cr}(V_{HV} - nV_{LV})} \quad (17)$$

In order to calculate D_F, we need to evaluate ΔV_{cr}. Due to the symmetric operation, i_{Lres} has no DC offset value and thus the average value of the current through resonant inductor is twice that of the high voltage side current.

$$I_{H\_V} = \frac{1}{T_{sw}}\left[\int_{t1}^{t2} \frac{r_1}{Z_r}\sin[\alpha + \omega_r(t - t_1)]dt\right] \quad (18)$$

$$I_{H\_V} = \frac{r_1}{T_{sw} Z_r \omega_r}\left[\cos(\alpha) - \cos\left(\alpha + \omega_r(t_2 - t_1)\right)\right] \quad (19)$$

Since $\alpha + \omega_r(t_2 - t_1) = \pi$, if the worst-case scenario i-e no dead band is considered. Then

$$2\Delta V_{cr} = r_1 cos(\alpha) + r_1$$

Thus, rearranging the relation for ΔV_{cr} yields,

$$\Delta V_{cr} = \frac{I_{HV}}{2C_r f_{sw}} \quad (20)$$

Putting the value of ΔV_{cr} in (17),

$$D_F = \frac{1}{nV_{LV}}\sqrt{V_{LV}\left(G_f - 2n\right) I_{HV} L_{res} f_{sw}} \quad (21)$$

Where $G_f = \frac{V_{HV}}{V_{LV}}$ is the forward gain of the converter. If we rearrange (21) and solve for G_f then corresponding forward gain in terms forward duty ratio is,

$$G_f = n\left(1 + \sqrt{1 + \frac{D_F^2 V_{HV}}{I_{HV} L_{res} f_{sw}}}\right) \quad (22)$$

Figure 3.5 is a three-dimensional surface plot created using MATLAB. The data for the plot was obtained by simulating the mathematical model of the bidirectional DC-DC converter, where key performance parameter such as forward duty ratio D_F , forward voltage gain G_f and output current on the high-voltage side P_{HV}were evaluated over a range of values. The x-axis represents the forward duty ratio (D_F), the y-axis represents the corresponding forward voltage gain G_f and the z-axis shows the resulting high-voltage side output current P_{HV}.

This graphical representation helps visualize how increasing the duty ratio leads to an increase in both voltages gain and output current capacity on the high-voltage side of the converter. The plot was generated using MATLAB's mesh grid and surf functions based on the equations derived from the converter's operating principles

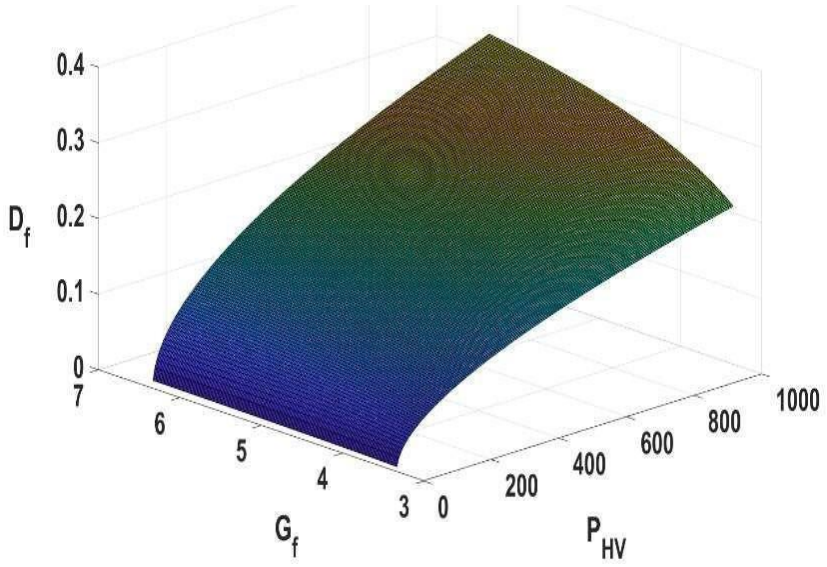

Figure 3.5: Impact of Output Power on Duty Cycle and Voltage Gain in Forward Mode

3.4 Design Guidelines

This section describes the design equations for the passive components of the proposed actively clamped bidirectional resonant NPC-type DC-DC converter.

3.4.1 Transformer Turns Ratio Determination

The voltage gains of the proposed converter in either V2G or G2V mode determine the turns ratio of the transformer i-e,

$$\frac{V_{\text{H\_V}}}{V_{\text{LV-min}}} \leq n \leq \frac{V_{\text{H\_V}}}{V_{\text{LV-max}}} \tag{23}$$

Where $V_{\text{LV-min}}$ and $V_{\text{LV-max}}$ are the minimum and maximum Low voltage side voltage levels respectively.

$$N_{\text{p}} \geq \frac{i_{\text{p\_k}} L_{\text{m}}}{B_{\text{m}} A_{\text{e}}} \times 10^4 \tag{24}$$

$$N_{\mathrm{p}} \geq \frac{30 \times 20 \times 10^{-6} \times 10^{4}}{0.1 \times 3.28} \quad (25)$$

$$N_{\mathrm{p}} \geq 20$$

$$N_{\mathrm{s}} \geq 20 \times 1.2 \geq 25$$

Where $N_P is\ the\ number\ of\ turns\ of\ primary\ side\ and\ N_s\ is\ the\ number\ of\ turns\ at\ secondary\ side.$

3.4.2 Magnetizing Inductance

The magnetizing inductance L_{m} directly corresponds to the ZVS behavior of the switch S_1. The duration t_{df} is the dead time at the start of the switching cycle in forward mode. These time durations are relatively smaller than the switching cycle T_{s} and thus the magnetizing current i_{Lm} can be considered constant. These constant current discharges the drain to source capacitance C_{DS1} of S_1 and charges the drain to source capacitance C_{DS} of S_2. The necessary condition for ZVS turn on of switch S_1 is given by,

$$2V_{LV}C_{DS1} < \left|\int_0^{t_{df}} ni_{Lm}(t)\,dt\right| = -nL_{L\_mf}t_{df} \quad (26)$$

0

I_{Lmf} acts as current source and is given by

$$I_{Lmf} = -\frac{nV_{LV}}{4L_m f_{sw}} + \frac{1}{2}I_{L\_V} \quad (27)$$

Substituting the value of I_{Lm} in eq (43) yields

$$L_m < \frac{n^2 V_{L\_V} t_{df}}{2nI_{LV}t_{df}f_{sw} - 8f_{sw}C_{DS1}V_{LV}} < 40uH \quad (28)$$

3.4.3 Resonant Inductor and Capacitor Selection

The resonant capacitors should not be fully discharged during the converter operation in both modes of operation. The constraints regarding resonant capacitor for stable operation of the converter are,

$$v_{Cr1}(t) > 0\ , v_{Cr2}(t) > 0 \quad (33)$$

$$\Delta v_{Cr} \geq \frac{V_H}{2} \quad (34)$$

Substituting (20) in (34) yields,

$$C_r \geq \frac{I_{H\_V}}{V_{H\_V}\, f_{Sw}} \geq 140nF \quad (35)$$

Where, $C_{r1} = C_{r2} = \frac{C_r}{2}$

The high output currents therefore mean high voltage ripple over the capacitor. In order to satisfy equation (35), one should choose the resonant capacitor high enough so that its value is such that.

Ripple is inversely related to Frequency. For given load current the voltage ripple decreases with increasing switching frequency. This is because the capacitor is more effective of smoothing the voltage because between switching cycles it has less time to discharge. Small ripple in the high voltage is achievable from higher switching frequency. Nevertheless, increased switching frequency affects other design aspects, including:

Switching losses: Higher frequencies can cause more switching losses and as a result reduce efficiency.

Size and cost of components: High-frequency operation might require smaller passive components, but it will increase the complexity.

Since $\omega_r = 1/\sqrt{LrCr}$, (35) implies,

$$L_r \leq \frac{V_{HV} f_{Sw}}{{\omega_r}^2 I_{HV}} \leq 140uH \quad (36)$$

Inductor value increases with increase in output current. While satisfying the equation, higher value of L_R should be selected

3.4.4 Closed Loop Control Design

In the Figure 3.6, the AI-based feedback control system for our isolated DC-DC converter in NPC topology is explained. It operates by continuously adjusting the duty cycle of its four switching devices in response to real-time system parameters, ensuring optimal power conversion. The Neural Network (ANN) is trained to predict the precise duty cycles required for each switch based on extracted system features such as input voltage (50V-70V), output voltage (380V), load current, and transient conditions. The feedback loop starts with real-time data acquisition from voltage and current sensors, which monitor fluctuations in system performance. This raw data is processed through a feature extraction module, which refines it into a structured form suitable for ANN input. The ANN, having been pre-

trained with datasets obtained from various operating conditions, uses this data to predict the optimal duty cycle values for the four switches of the NPC isolated DC-DC converter. Unlike a conventional PID controller, which relies on a fixed proportional-integral-derivative response that struggles with nonlinearities, dynamic loads, and sudden transients, the ANN is adaptive and data-driven, making it more effective at minimizing voltage ripples, overshoot, and steady-state errors. The ANN model understands multiple input parameter relationships thus enabling proactive action instead of target-based reaction. The ANN uses studied data on required adjustments for predictive control which enables it to make corrections that surpass PID controller's reactive methodology. The system obtains quicker reference voltage attainment and establishes better stability when encountering situations like abrupt load alterations or supply voltage changes or switching events through this approach. The distribution method of duty cycle by the ANN across the four switches in the NPC topology precisely controls voltage distribution for optimal efficiency and reduced switching losses. The AI-based method obviates the requirement for human-generated PID gain adjustments while boosting the performance level of DC-DC converters operating in high power density applications with dynamic needs.

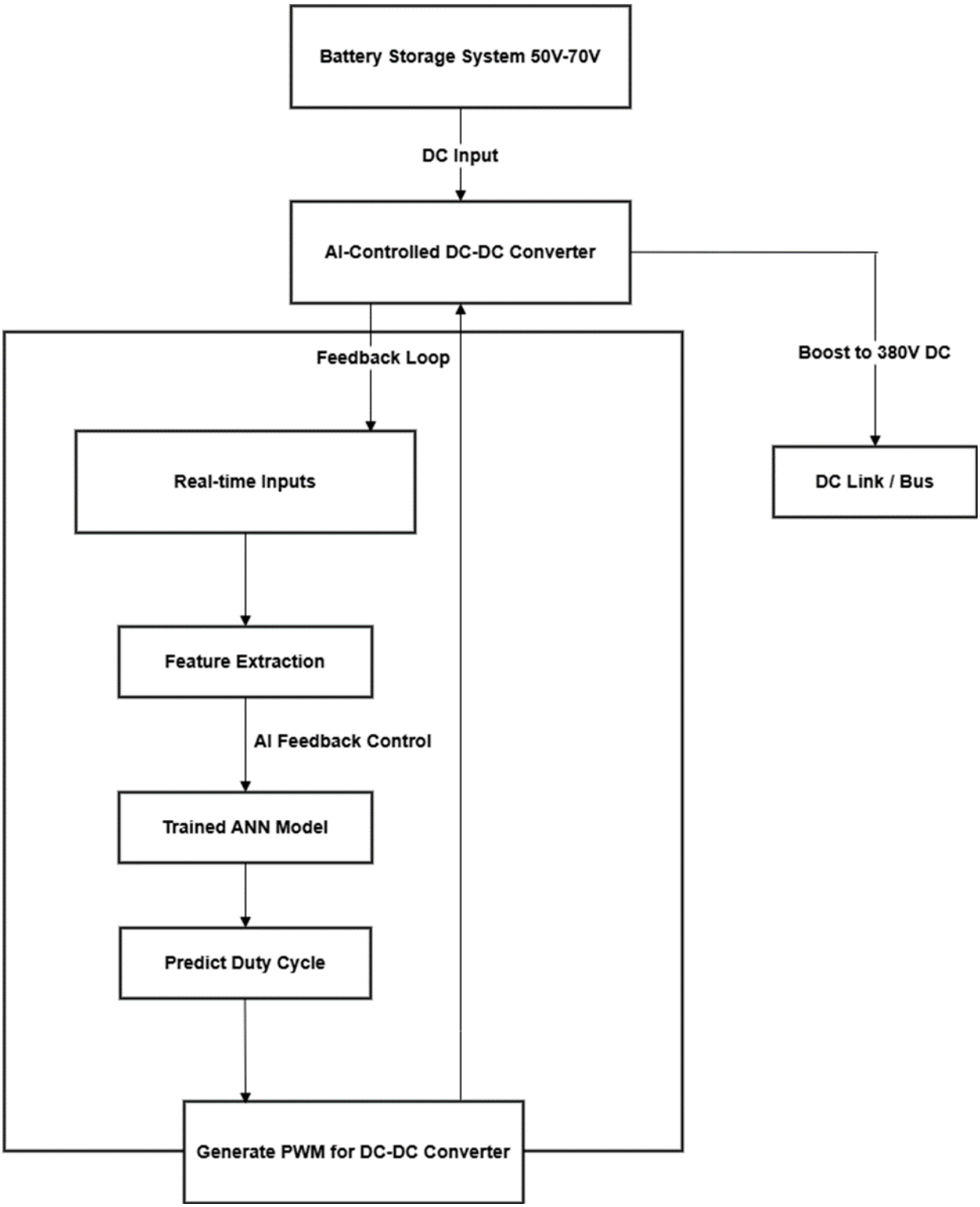

Figure 3.6: Closed Loop Control Design of DC-DC converter using ANN control

3.5 Data Collection and Simulation Setup

The initial step of developing an Artificial Neural Network (ANN)-based duty cycle predictor for our isolated DC-DC in NPC topology converter includes establishing MATLAB/Simulink simulations to generate data from different operating situations. The training of the ANN model needs the essential data for replacing traditional PID controllers with predictive control technology. The implementation of the data collection method and simulation process follows these main operational procedures:

3.5.1 MATLAB/Simulink Simulation Setup

A complete isolated DC-DC converter in NPC topology and control feedback mechanism along with control logic are integrated in the MATLAB/Simulink simulation model. The simulation platform duplicates actual power converter operations for diverse operating scenario data collection purposes.

3.5.2 Simulation Components

The simulation consists of:

Power Stage (NPC DC-DC Converter): Includes MOSFETs, diodes, inductors, and capacitors. Controller (PID/ANN-based): Initially, a PID controller is used for data collection before transitioning to ANN-based control.

Sensors and Measurement Blocks: To capture real-time voltage and current waveforms. Data Logging Mechanism: Stores simulation results for ANN training.

3.5.3 Converter Parameters

The isolated DC-DC converter in NPC topology is designed to operate under the following conditions:

Table 3.1: Control parameters of NPC DC-DC converter with ANN Feedback

Sr. No	Parameter	Value
1.	Input Voltage (Vin)	50V - 70V
2.	Output Voltage (Vout)	380V
3.	Switching Frequency	50 kHz - 100 kHz
4.	Load Variations	10% to 100% of rated power

The simulation is run under different conditions to ensure comprehensive data collection.

3.5.4 Operating Conditions for Data Collection

I. No -Load Condition

The converter operates with No load. The controller maintains output voltage stability with minimal duty cycle adjustments. Data is logged to observe control behavior at low-power conditions.

II. Full-Load Condition

The converter is operated at maximum load (rated output power).

High current is drawn from the source, affecting the duty cycle and transient response. The response time of the PID controller in maintaining steady-state voltage is recorded.

III. Light Load Condition

The converter operates with minimal load. The controller maintains output voltage stability with minimal duty cycle adjustments. Data is logged to observe control behavior at low-power conditions.

IV. Varying Load Condition

Load is suddenly increased or decreased to simulate real-world disturbances. The PID controller adjusts the duty cycle, but with some delay and overshoot. This data is crucial for training the ANN to predict duty cycles with better transient handling as shown in Figure 3.7.

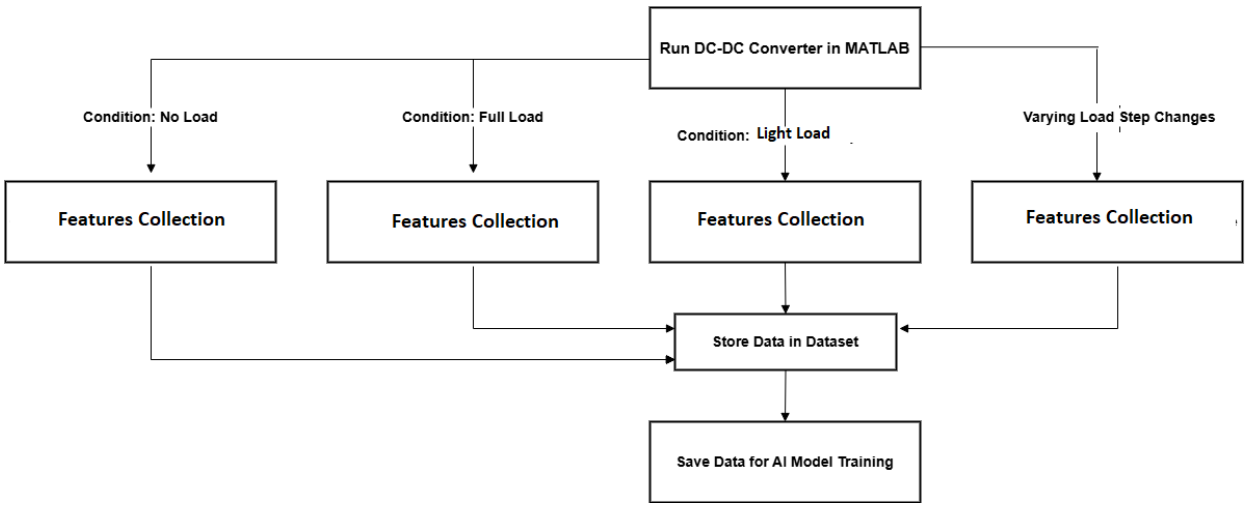

Figure 3.7: Data Set Collection on Load Transients

3.5.5 Data Collection from PID-Controlled System

To train the ANN, extensive data is collected from the PID-controlled converter under the above operating conditions. The data consists of inputs and output signals, which the ANN will later use to predict optimal duty cycles as illustrated in Figure 3.8.

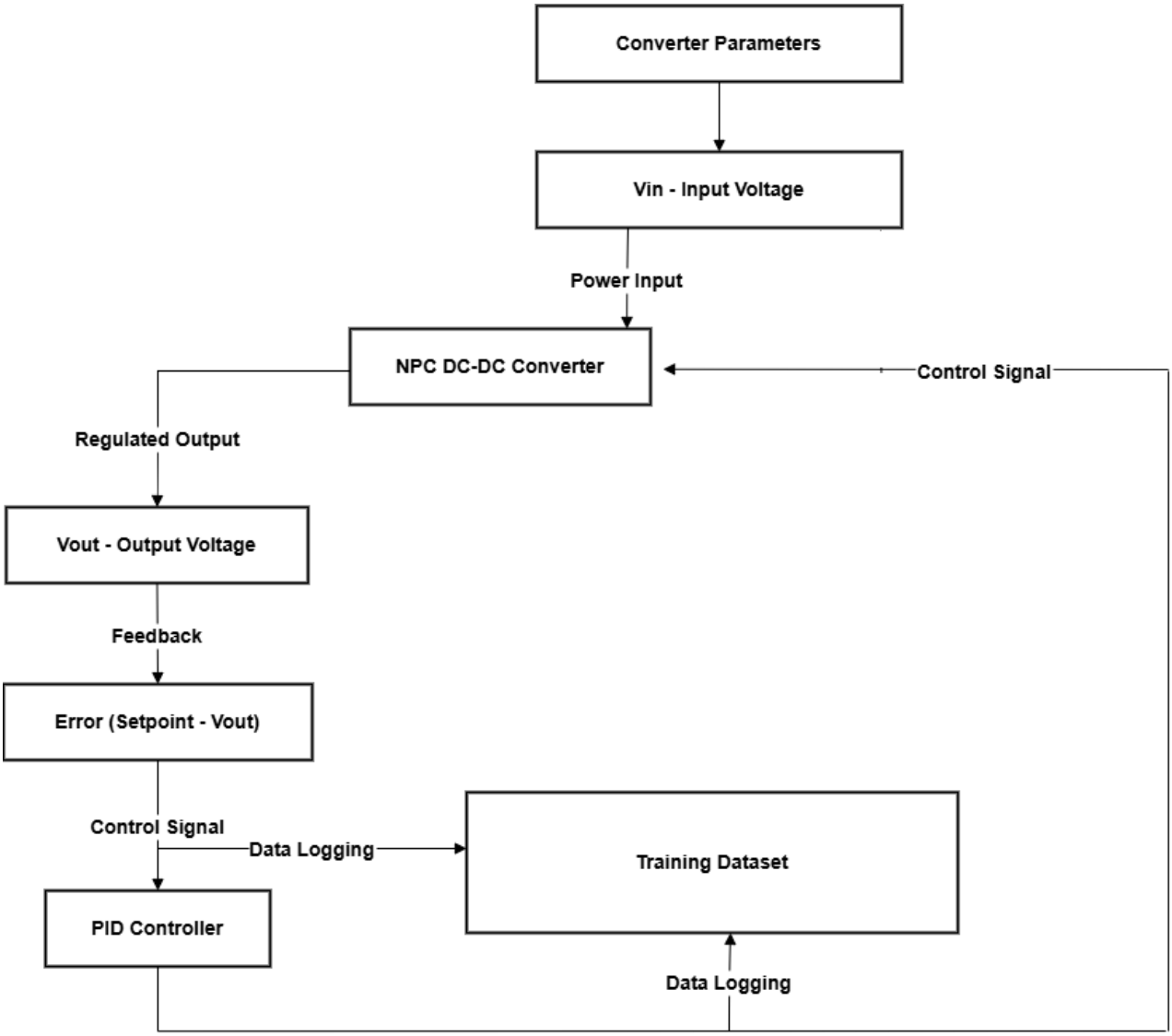

Figure 3.8: Training of ANN on PID Feedback Control Data

3.5.6 Input Parameters (Features for ANN)

Supplied Voltage (Vin) stands as the main input affecting the converter. Power demand appears through Input Voltage (V_{in}) while the converter pulls this current from the source. Output Voltage and output current ($V_{out,}$ I_{out}) serves to display changes in the load which impact control system performance. The PID controller uses Error Signal (Error = Setpoint - V_{out}) to determine the essence of output voltage versus target voltage differences and Error is names as control and predicted result from PID is treated as response and ANN is being trained on these features and later was trained in unseen signals.

3.5.7 Output Parameter (Target for ANN)

Duty Cycle (D) serves as the main control parameter for the switching sequence of the four MOSFETs in an NPC DC-DC converter. Each dataset contains time-series data records of (Error = Setpoint - V_{out}) and response that will be utilized in ANN model training in order to generate Duty Cycle.

3.6 ANN Training & Implementation

The training and testing dataset selection occurred according to operational data collection conditions instead of employing random partitioning. Stable performance data measured under the conditions of no load and light load and random load and full load operations served as input for training the Artificial Neural Network (ANN). The selected conditions allowed the ANN to learn the specific control behavior that matches expected functions during regular converter operation. The reserve data set contained all sudden and dynamic load variations since they were absent from the training dataset. The training process permitted the ANN to learn standardized controlled patterns yet its performance evaluation focused on generalization abilities for unpredictable transient operational situations. A distinction between training and testing data sets emerged from the selection standard that consisted of using steady-state data for training while dynamic load transition data served for testing purposes. The entire training validation deployment procedure appears as Figure 3.10 illustrates.

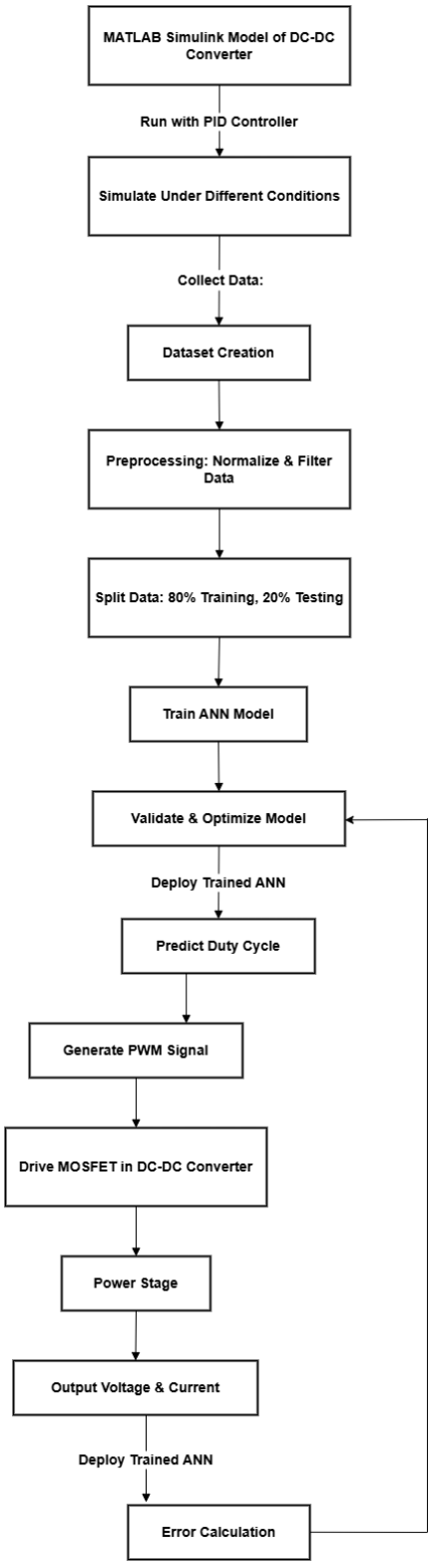

Figure 3.9: Flow of ANN Training on PID & Real time Implementation

The Feedforward Neural Networks (FNN) for designing the DC-DC converter controller is used. The selection of this architecture hinged on its ability to perform high-quality approximations. ANN technology substituted the conventional PID controller structure.

3.7 Architecture of ANN

The feedforward architecture of the ANN consisted of three primary layers:

Input Layer: Receives system parameters such as input voltage, input current, output current, and error.

Hidden Layers: Process the input signals through nonlinear activation functions, extracting relevant features for accurate duty cycle prediction.

Output Layer: Produces the predicted duty cycle, which is then used to control the switching of the MOSFETs in the converter.

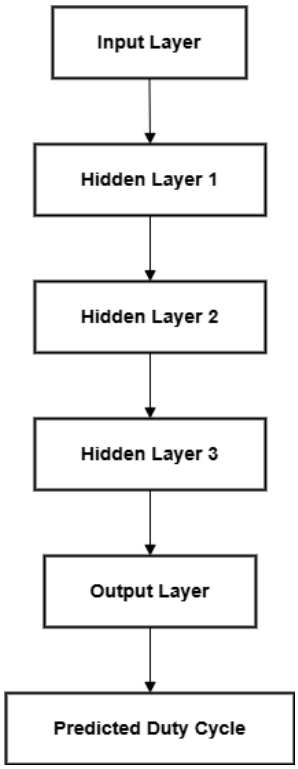

Figure 3.10: Architecture of ANN

3.7.1 Input Layer

The input layer consisted of four key parameters that significantly impact the operation of the DC-DC converter:

Vin (Input Voltage): Indicates the voltage supplied to the converter. Variations in Vin influence the required duty cycle.

Iin (Input Current): Provides information about power drawn from the source.

I_{out} (Output Current): Represents the load current demand.

Error (Setpoint - Vout): The difference between the reference voltage and the actual output voltage, used to adjust the duty cycle.

3.7.2 Hidden Layers

The hidden layers in the feedforward ANN process the input data through neurons that apply activation functions to introduce non-linearity into the model.

Number of Neurons

The number of neurons in each hidden layer was determined through experimentation, ensuring balance between computational complexity and performance. Too few neurons lead to underfitting, while too many cause overfittings.

Activation Functions

Each neuron in the hidden layers applies a Rectified Linear Unit (ReLU) activation function, defined as:

$$\mathbf{f(x) = max(0, x)} \tag{37}$$

This function is computationally efficient and helps prevent the vanishing gradient problem, allowing deeper networks to be trained effectively.

Weights and Biases: Each neuron has trainable weights and biases that adjust during training to minimize prediction error.

3.7.3 Normalization and Preprocessing

Before training the ANN, the input data is normalized to improve convergence and prevent large variations in numerical values.

$$X_{norm} = \frac{X - X_{min}}{X_{max-}X_{min}} \quad (38)$$

Where,

$\boldsymbol{X_{norm}}$ is the Normalized value

$\boldsymbol{X}$ is the raw input value

$\boldsymbol{X_{max}}$ and $\boldsymbol{X_{min}}$ is the raw input value is the main and max values in datasets

3.7.4 Loss Function and Optimization Technique

ANN is trained using supervised learning, where the loss function determines the difference between predicted and actual duty cycle values.

$$\text{Mean Square Error (MSE)} = \frac{1}{N}\sum_{i=1}^{N}\left(D_{pred} - D_{actual}\right)^2 \quad (39)$$

$\boldsymbol{D_{pred}}$ is the predicted duty cycle.

$\boldsymbol{D_{atual}}$ is the actual duty cycle obtained from the PID-based system.

$\boldsymbol{N}$ is the total number of samples.

3.7.5 Final Output Layer

The output layer consists of a single neuron that predicts the required duty cycle (DDD) for controlling the DC-DC converter. The activation function f(x) used in the output layer is typically Sigmoid or Linear:

$$\text{f(x)} = \frac{1}{1 + e^{-x}} \quad (40)$$

This ensures that the output remains in the range **(0,1)**.

3.7.6 Activation Functions

Activation functions are a vital part of feedforward neural networks (FFNNs), allowing them to approximate complex nonlinear functions. By introducing non-linearity, these functions enable the network to learn intricate relationships between inputs and outputs, which is essential for controlling the duty cycle in DC-DC converters under various operating conditions.

In this thesis, the FFNN was trained using a combination of three commonly used activation functions: tansig, logsig, and purelin, each serving a specific role in the network's architecture.

3.7.6.1 Hyperbolic Tangent Sigmoid Function (tansig)

The tansig function introduces non-linearity and maps the input to the range (–1, 1). It is particularly useful in hidden layers for faster convergence due to its zero-centered output.

$$\mathbf{f(x) = tanh(x) = \frac{2}{1+e^{-2x}} - 1} \quad (41)$$

3.7.6.2 Logarithmic Sigmoid Function (logsig)

The logsig function squashes input values into the range (0, 1), making it ideal for normalized data and network stability in early layers.

$$\mathbf{f(x) = \frac{1}{1+e^{-x}}} \quad (42)$$

3.7.6.3 Linear Activation Function (purelin)

The purelin function is a linear activation function that outputs the input without modification. It is typically used in the output layer of regression-based neural networks.

$$\mathbf{f(x) = } x \quad (43)$$

3.8 Control Logic Flowchart and Pseudocode

In this section the overall control logic of the ANN based system has been described which is used to predict duty cycle in the proposed converter. Data loading creates the flow which leads to training of ANN models using different activation functions and finally testing the flow along with ripple performance analysis.

The whole process starts with 'Start' node that leads us to the loading of training datasets. Following that, `tansig`, `logsig` and `purelin` are defined as activation functions. Then the system goes for a training loop where at each instance of a case, it initializes an artificial neural network (ANN) with 5 neurons, then trains using the `trainlm` algorithm. First, all datasets are trained sequentially on the networks and the trained models are saved to disk. Then, training is completed, and the test dataset as well as the PID dataset are loaded. After that the duty cycle predictions are made and the output voltage (Vout) interpolated from it. The Results, Vin, Iout, Vmax, Vmin, Vavg, all these results are compared to calculated ripple at Vin, and are then plotted, calculating Vout from PID Vout and ANN Vout. In this case, loop repeats once for each ANN, and a ripple comparison table is displayed and the process ends as shown in the Figure 3.11.

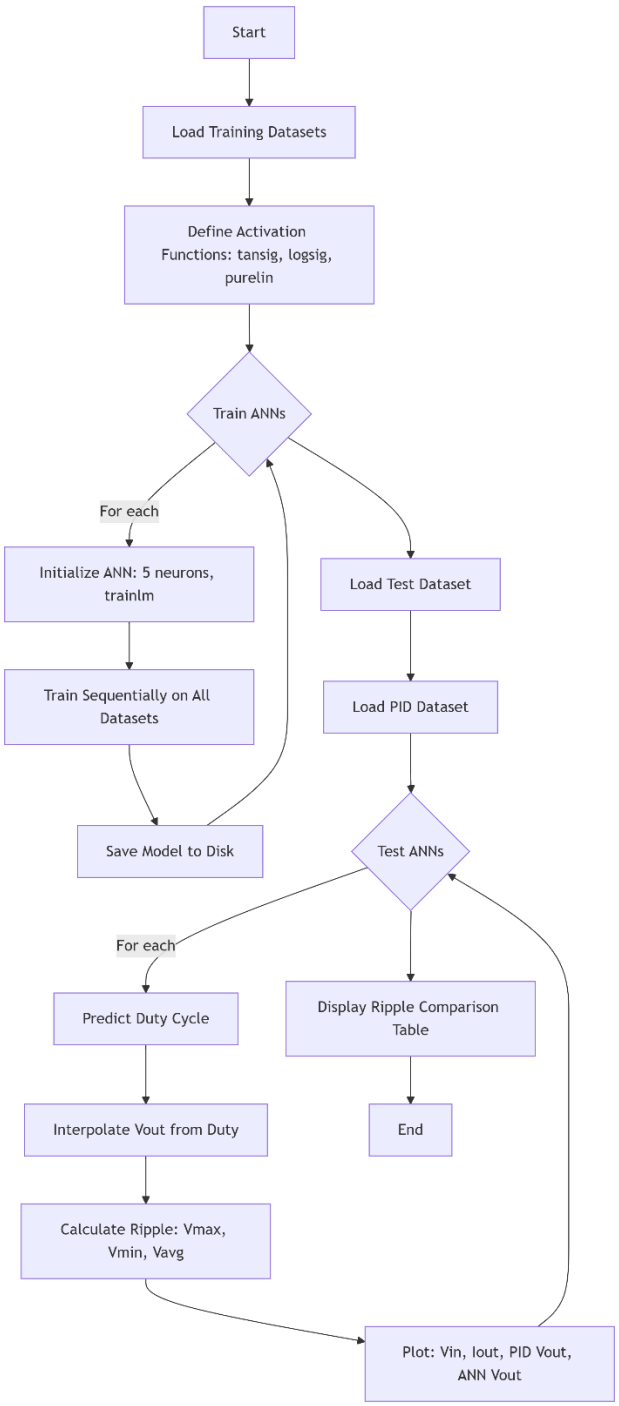

Figure 3.11: Flowchart of MATLAB Code for Training, Testing, Validation and Results visualization of ANN control for NPC DC-DC converter

3.8.1 Pseudocode of the Control Logic

```
BEGIN MAIN FUNCTION
DEFINE datasets = list of training datasets
DEFINE test Dataset = selected test dataset
DEFINE activation Functions = {'tansig', 'logsig', 'purelin'}
FOR each activation function in activation Functions DO
    LOAD all training datasets
    FOR each dataset:
        EXTRACT input-output pairs for training
    END FOR
    INITIALIZE ANN with specified activation function
    TRAIN model sequentially on all datasets
    SAVE trained model to disk
    LOAD trained model into MATLAB workspace
END FOR
LOAD test dataset
LOAD PID dataset for comparison
FOR each trained ANN model:
    PREDICT duty cycle using test input data
    INTERPOLATE predicted output voltage (Vout) based on duty prediction
    COMPARE ANN-predicted Vout with PID Vout
    CALCULATE ripple: Vmax, Vmin, Vavg, ripple, ripple %
    PLOT Vin, Iout, PID Vout, ANN Vout
    RECORD ripple results in table
END FOR
DISPLAY ripple comparison table
END MAIN FUNCTION
```

CHAPTER 4: SIMULATION AND RESULTS

The chapter presents the evaluation of PID controllers alongside ANN-based controllers occurred through simulation. The research applied an ANN-based controller for operation of the isolated DC-DC converter in Neutral Point Clamped (NPC) topology. The main objective is to assesses the performance of ANN compared to standard PID controller in achieving better results in terms of output voltage ripple, transient response under load variations, and robustness against input voltage fluctuations. The research contains simulation results of comparison of both converters. The entire content in this chapter derives from MATLAB/Simulink-based simulation work. The simulation setup validated the performance assessment by implementing identical operating environments for testing the controllers for accurate and fair comparison.

4.1 Voltage to Grid Mode Results

The power converter was simulated in MATLAB SIMULINK in forward mode where it stepping up the voltage and working as a Boost converter as shown in Figure 4.1.

Artificial Neural Network (ANN) is trained using real-time data collected from the converter operating under various conditions, including disturbances, load variations, and dynamic changes in input voltage. The training dataset includes system responses when controlled by a PID controller, capturing both steady-state and transient behaviors. Once trained, the ANN is integrated into the control loop, replacing the traditional PID controller to regulate the output voltage. The ANN processes real-time inputs such as voltage, current, and error signals and predicts the optimal duty cycle for the switching signals, ensuring stable and adaptive control. The ANN's response is then compared against the PID-based control in terms of voltage regulation, transient response, overshoot, steady-state error, and adaptability to disturbances. Results indicate that the ANN-based controller provides faster dynamic response, reduced overshoot, lower steady-state error, and better robustness to disturbances, demonstrating its superiority over conventional PID control in NPC converters.

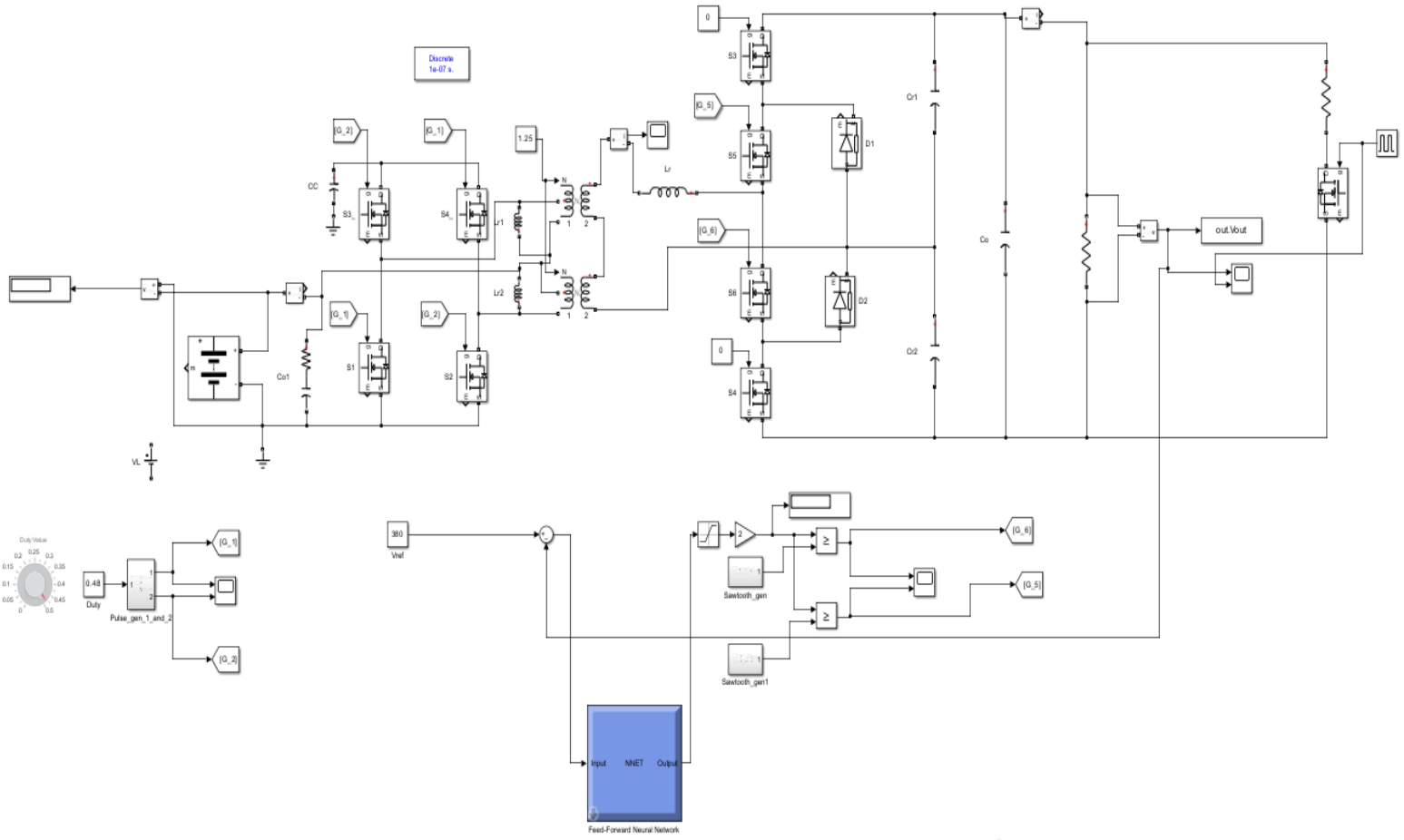

Figure 4.1: NPC Converter Schematic with ANN Feedback Control

4.2 Simulation Results:

A detailed Simulink model became the first necessary step for evaluating controller performance model of our isolated DC-DC Converter in NPC topology. The converter included multiple semiconductor parts. An efficient output voltage regulation happens when switches work at high switching frequencies to regulate output voltage. The Wider testing conditions included voltage input and output levels and load specifications which experienced real-world conditions. scenarios. The control system functioned as the fundamental component for changing the converter's duty cycle operation. The system utilizes switching elements which control output voltage stability. The PID controller usually received its design from conventional approaches with Ziegler-Nichol's method combined with additional fine-tuning. The control law for the PID system the control system used duty cycle adjustment through three elements where proportional and integral and derivative aspects governed the duty cycle's modifications depending on output voltage changes. deviation of the output voltage from the reference value. However, despite careful tuning, the PID the controller displayed specific drawbacks in its capacity to deal with abrupt changes in the load and maintain low output voltage ripple. suppressing output voltage ripple effectively. The ANN-based controller functioned as a real-time device which predicted instantaneous optimal duty cycle values. based on multiple system parameters. The ANN received supervised training following which it learned to generate results. Several simulation conditions along with differing load circumstances and input conditions constitute the training set for dataset development. voltage variations. The ANN received four main input features that integrated voltage error together with the current value of the duty cycle combined with output current and input voltage. output current, input voltage, and previous output voltage. The parameters used for training enabled the ANN adjusted duty cycles in real-time thus delivering better system performance. over traditional PID control.

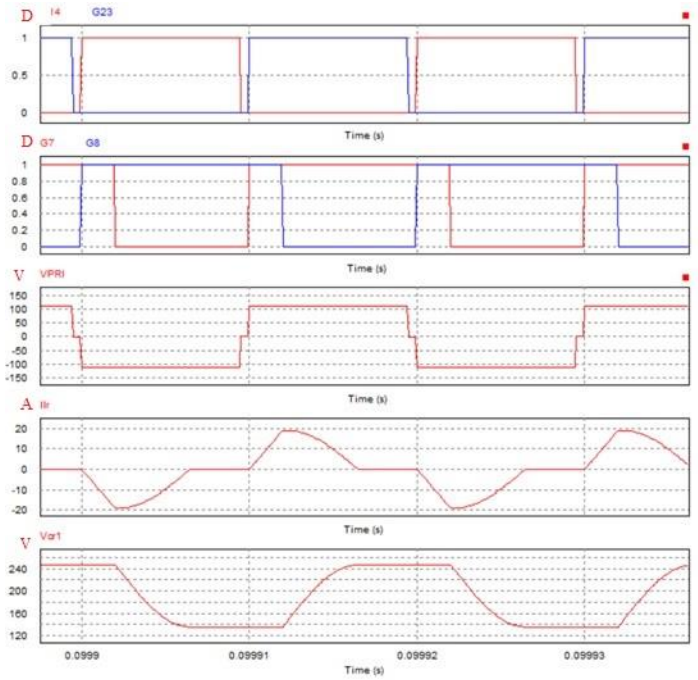

(a)

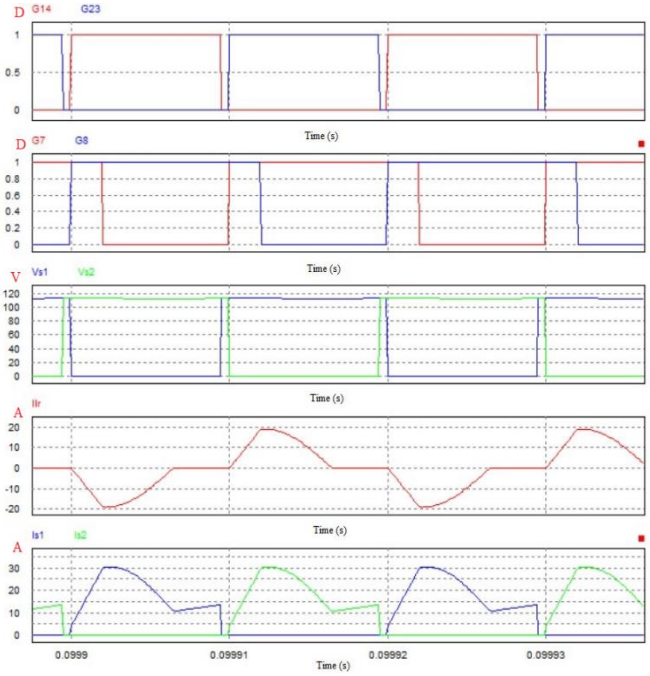

(b)

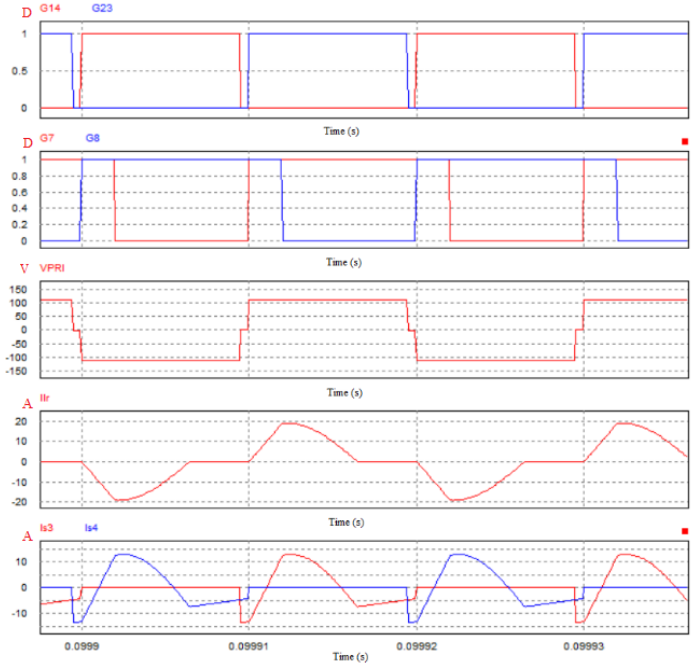

(c)

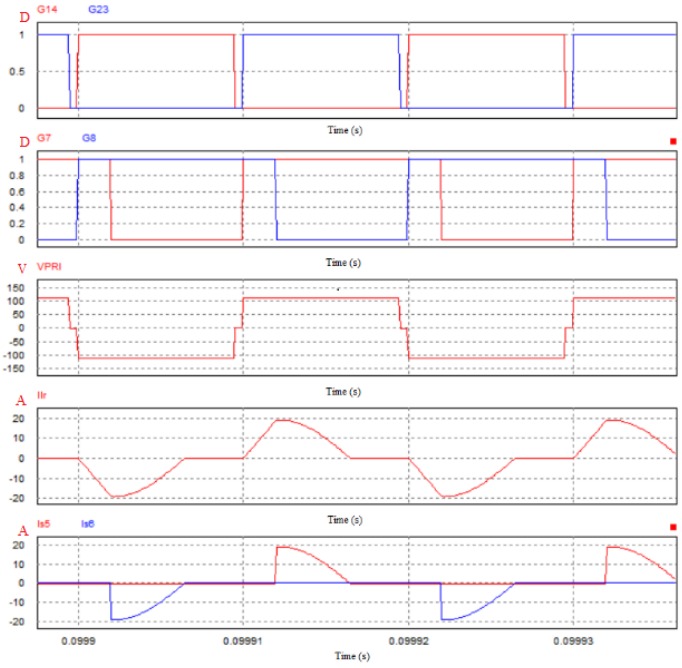

(d)

Figure 4.2: Gate signals on each Mosfet (a) v_{pri}, i_{Lr}, vcr1 (b) v_{s1}, i_{Lres}, i_{lr1}, i_{s1} (c) vpri, i_{Lr}, is3 (d) v_{pri}, i_{Lr}, i_{s5}

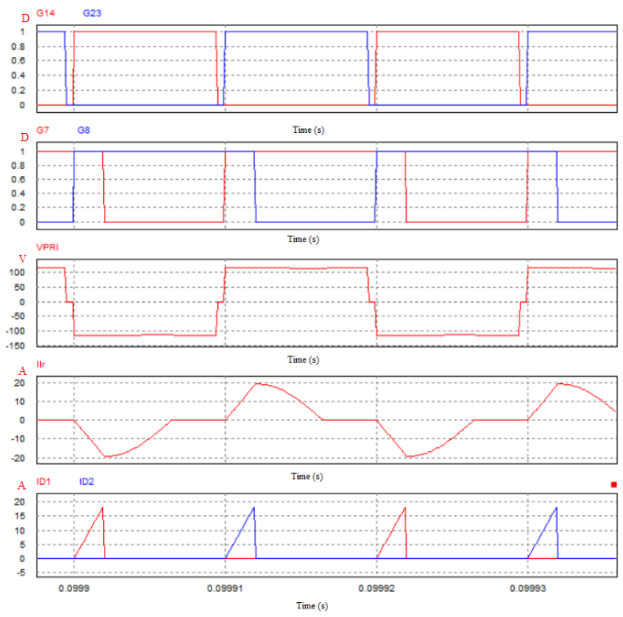

(c)

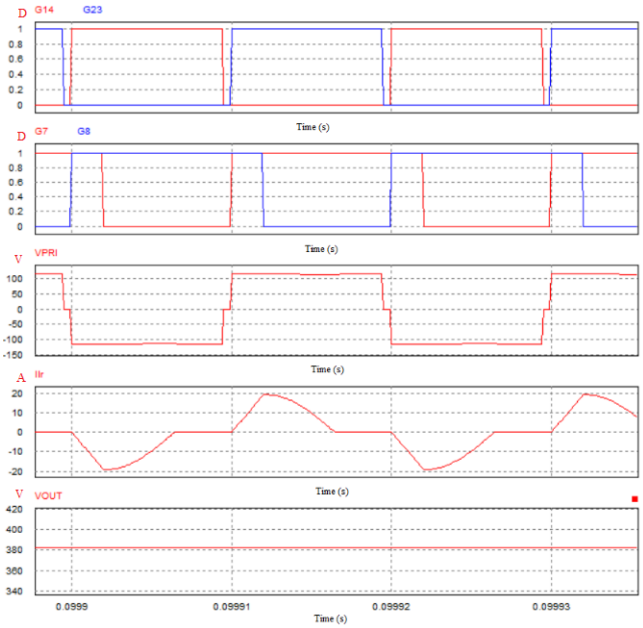

(d)

Figure 4.3: Simulation Results of Converter in Forward Mode.

In Figure. 4.2 (a), (b), (c), (d), and Figure. 4.3 (a), (b), the waveforms of the gating signals are provided to help readers better understand the modes of operation and the state of the converter. In addition to the gating signals, Fig. 28 (a) displays the waveforms of V_{pri} (primary voltage), i_{Lres} (resonant inductor current), and Cr1 (voltage across capacitor Cr1. When switches S5 and S6 turn on, the magnetization current Im begins to increase linearly, causing the primary voltage to rise to VLV. During the positive cycle, the current i_{Lres} increases linearly in the positive direction due to the clamping action of diode D2, while in the negative cycle, i_{Lres} increases linearly in the negative direction due to the clamping action of diode D1, as illustrated in Figure. 4.2 (a). When S6 turns off, the current i_{Lres} drops sinusoidally to zero, charging capacitor Cr1 to its maximum value.

The turn-on event of S1 achieves Zero Voltage Switching (ZVS), as shown in Figure. 4.2(b), due to the negative current flowing through the body diode DS1 and the discharge of the drain-to-source capacitance CDS1 during the dead time t_{Df}. After S6 turns off, the current flows through the body diodes of S3 and S5 during the positive cycle. Similarly, during the negative cycle, when S5 turns off, the current flows through the body diodes of S4 and S6, as depicted in Figure. 4.2 (c) and Figure. 4.2 (d), demonstrating the converter's ability to maintain stable operation and deliver the desired output. These waveforms collectively provide a comprehensive understanding of the converter's behavior across different modes of operation.

4.3 Performance Evaluation and Comparative Analysis

The investigation of the ANN-based controller effectiveness required simulations to be performed through different scenarios. The study began with performance tests on steady-state conditions by measuring output voltage ripple during continuous loads. Then next evaluation method examined the load transient behavior to assess controller adaptation speed during sudden changes in load level.

4.3.1 Steady-State Performance: Output Voltage Ripple Analysis

Any power converter must have a high rating for stable output voltage performance while minimizing output voltage fluctuations also named ripple. Simulation outputs showed PID-controlled system output displayed greater voltage spikes because its main reaction method depended on previous errors instead of predicting changes. The PID controller exhibited an essential operational weakness that prevented it from delivering consistent output voltage results when handling minor disturbances which caused detectable voltage fluctuations. The ANN-based controller achieved superior reduction of output voltage ripple through its real-time adjustments of the duty cycle. ANN achieved better performance due to its ability to use learning from various system parameters which let it predict system changes before large oscillations started. The implementation of ANN-based control resulted in substantial improvement of the output voltage profile by lowering its ripple level far beneath PID control performance metrics Figure 4.4 and Figure 4.5. The system stability received a boost as well as downstream component stress was reduced through the lower ripple levels in this practical power electronics application.

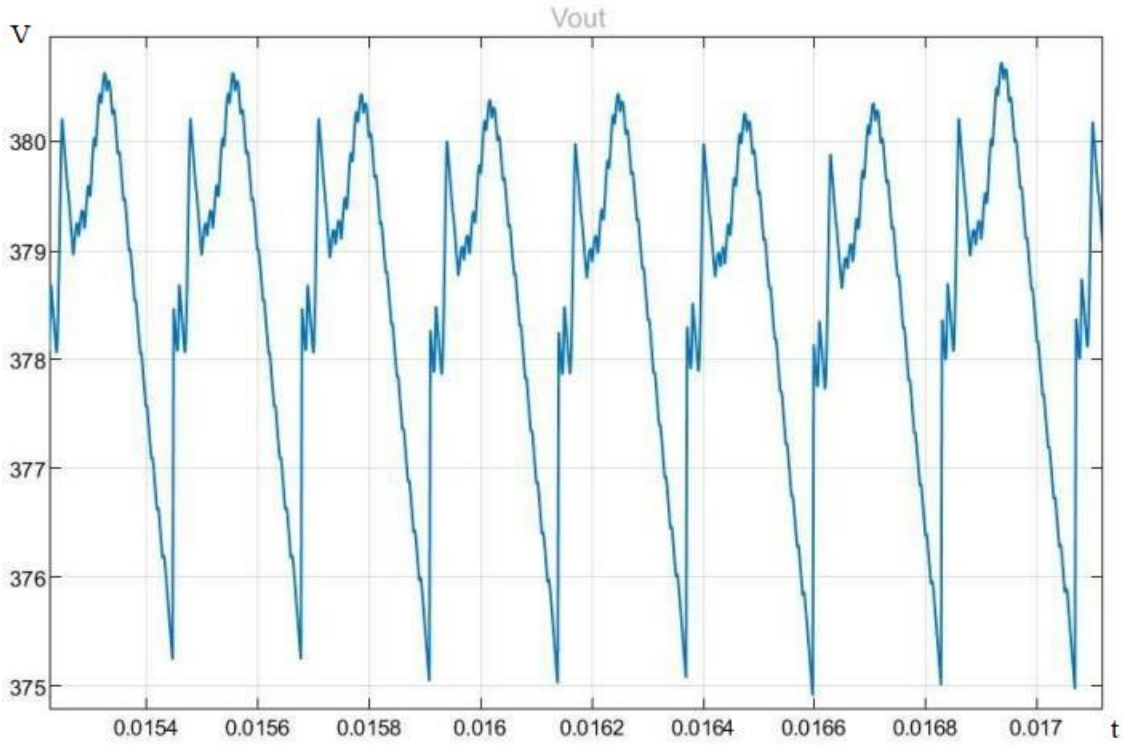

Figure 4.4: Output Ripple Voltage with ANN Feedback Control

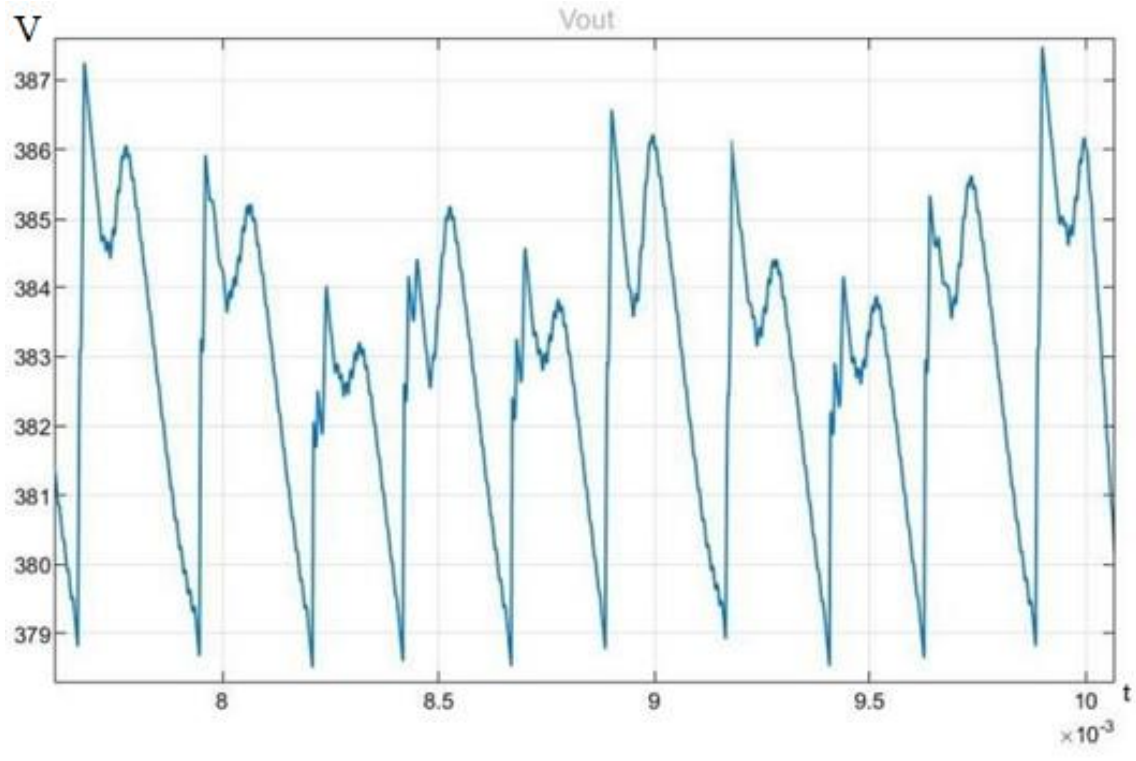

Figure 4.5: Output Ripple Voltage with PID Feedback Control

The ripple percentage is a key parameter in evaluating the performance of a control strategy for a DC-DC converter and will be calculated with below formula:

$$\text{Ripple (\%)} = \frac{(\text{Vmax} - \text{Vmin})}{Nomainal\ Voltage} \times 100$$

ANN Ripple Calculation:

$$\text{Vmax} = 380.7$$
$$\text{Vmin} = 375.2$$

Nomainal Voltage =380:

$$\text{Ripple (\%)} = \frac{(380.7 - 375.2)}{380} \times 100$$
$$\text{Ripple (\%)} = \frac{(5.5)}{380} \times 100$$

$$\text{Ripple (\%)} = 1.45\%$$

PID Ripple Calculation:

$$\text{Vmax} = 387.2$$
$$\text{Vmin} = 378.8$$

Nomainal Voltage =380:

$$\text{Ripple (\%)} = \frac{(387.2 - 378.8)}{380} \times 100$$
$$\text{Ripple (\%)} = \frac{(8.4)}{380} \times 100$$

$$\text{Ripple (\%)} = 2.21\%$$

Table 4.2: Comparison of Ripple Voltage of ANN and PID

Sr. No	ANN Ripple	PID Ripple
1	$\mathbf{1.45}\%$	$\mathbf{2.21}\%$

4.3.2 Load Transient Response: Performance Under Sudden Load Changes

The control system must feature proper design to minimize both overshoots and undershoots and settling time responses which occur due to sudden load variations. The simulation included a step load change that applied quick load increases followed by quick load decreases. Both controllers were studied for their capability to return output voltage back to its target value. The PID controller demonstrated large fluctuations of output that occurred during load transitions. The system took too long to adapt to

increasing demand thereby causing output voltage fluctuations until it regained stabilization. The PID controller demonstrated slow response during settling time because it needed extra time to revert the voltage to its reference value. The predictive derivative part of the PID control system could not adjust dynamically to changing load conditions because PID parameters remain static. The ANN-based controller exhibited stronger abilities in handling rapid change responses than alternative controllers PID did Figure 4.6, Figure 4.7 and Figure 4.8. The predictive intelligence of ANN operated rapidly upon load condition changes thus reducing voltage deviation levels. The system achieved stability rapidly after reaching lower levels of undershoot and overshoot with control performed through ANNs compared to PID control. Real-time adjustments from the ANN occurred because it learned from past load variations which improved its capability to adapt to sudden changes. The performance advantage from using ANN control matters most to power electronics applications because abrupt load changes need quick system responses to prevent instability or equipment breakdown.

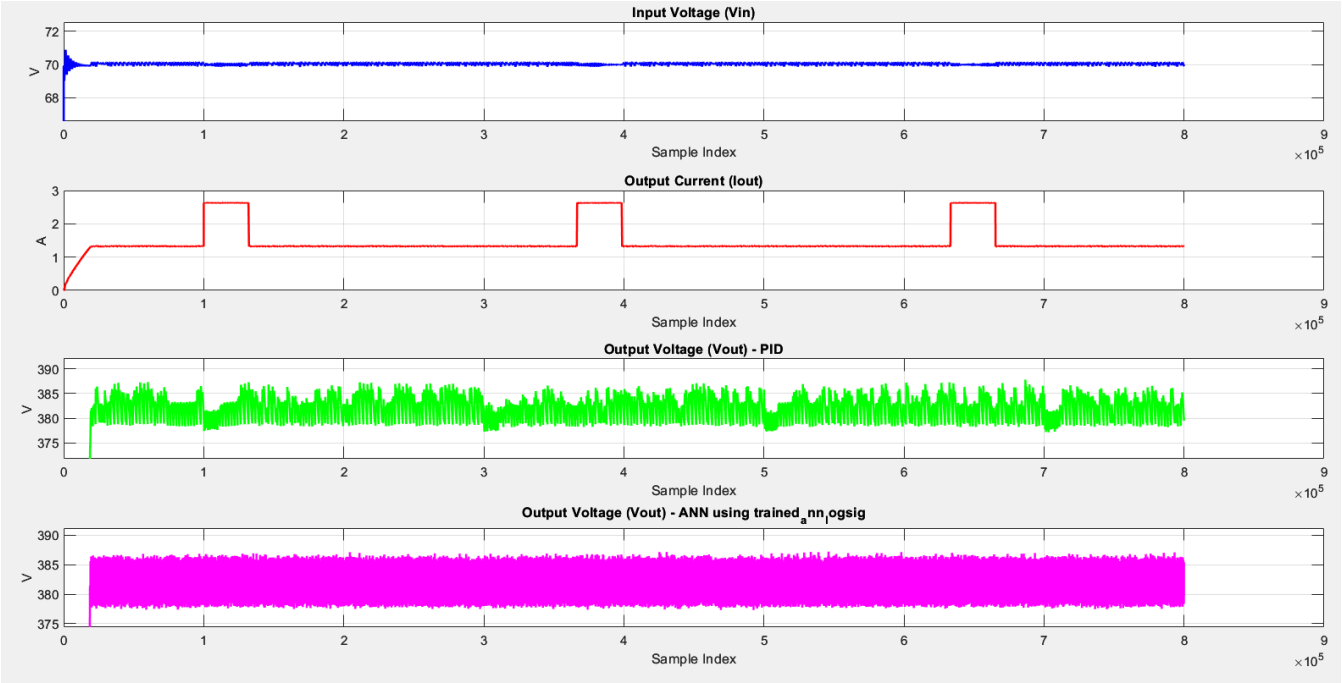

Figure 4.6: Voltage Response of PID and ANN (Activation Function: logsig) on sudden load transients

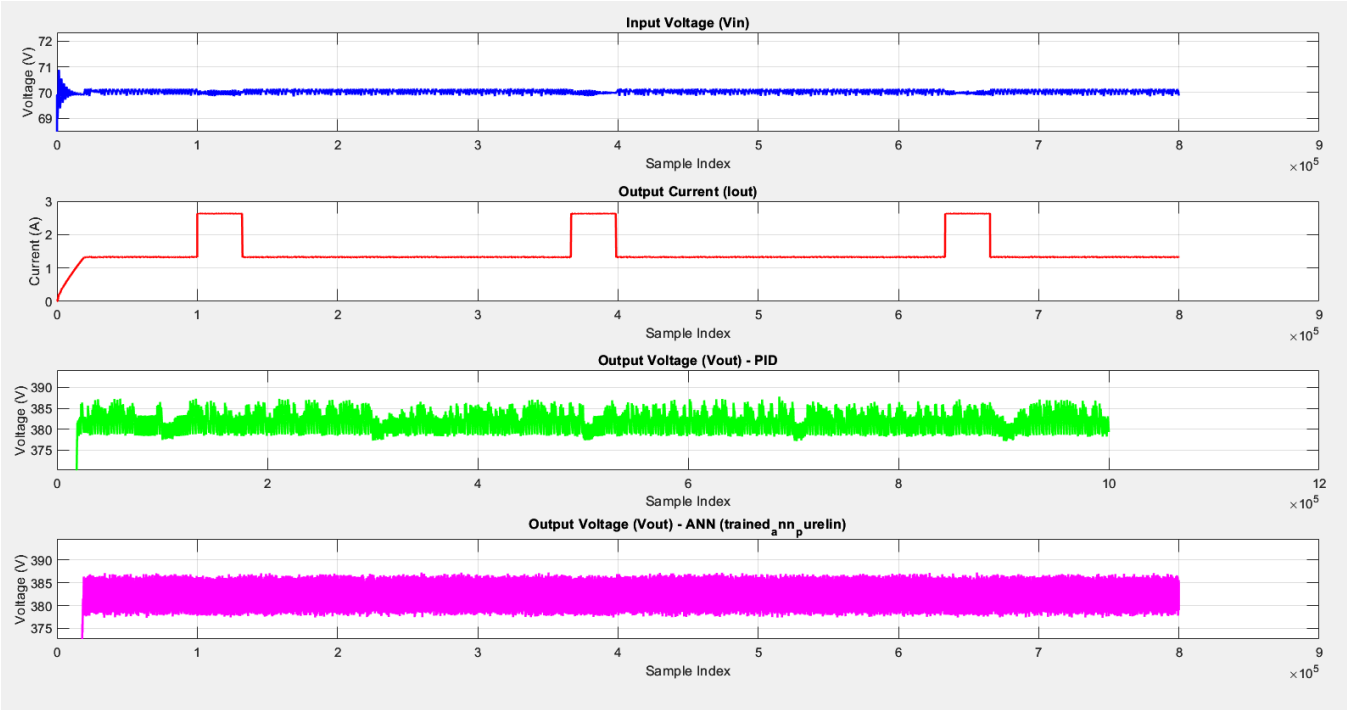

Figure 4.7: Voltage Response of PID and ANN (Activation Function: purelin) on sudden load transients

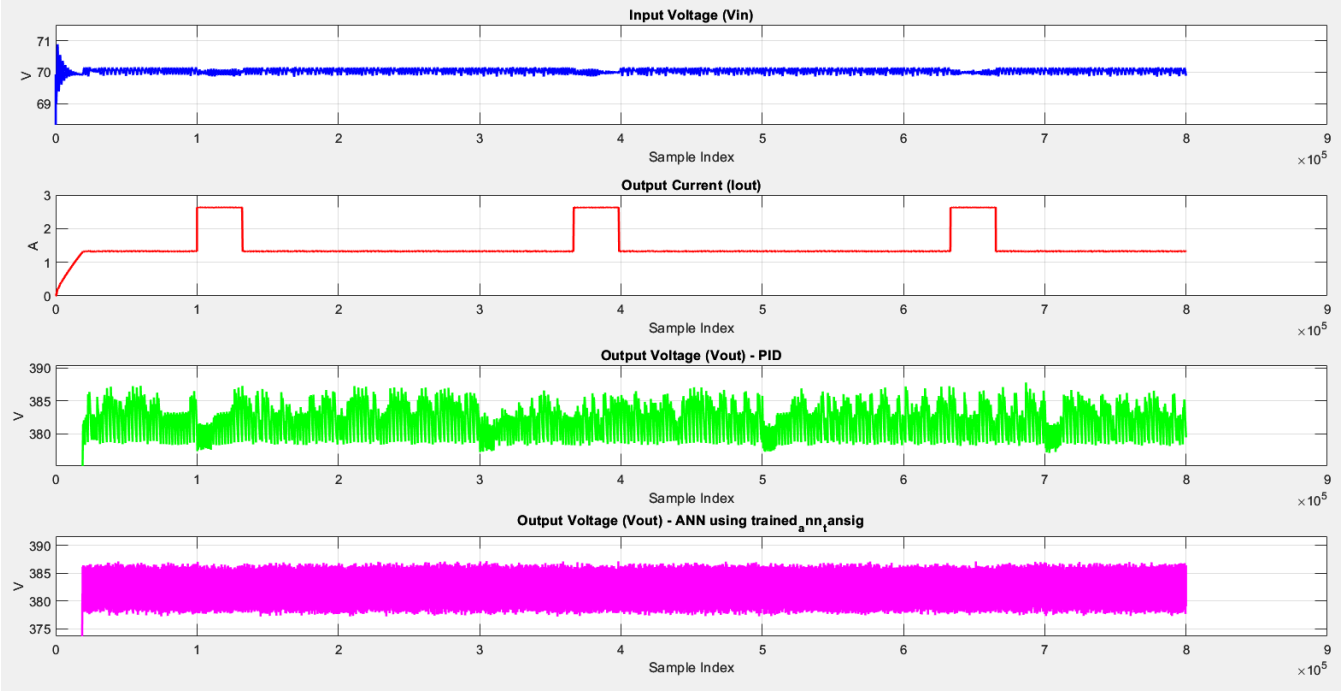

Figure 4.8: Voltage Response of PID and ANN (Activation Function: tansig) on sudden load transients

Similar to ripple the systems stability on load transients is also a key parameter in evaluating the performance of a control strategy DC-DC converter and will be calculated with below formula with $V_{Nominal}$=380V:

$$\text{Fluctuations (\%)} = \frac{(V_{NL} - V_{FL})}{V_{Nominal}} \times 100$$

Table 4.2: Absolute Ripple Voltage Comparison of ANN and PID

ANN Fluctuation with logsig Activation Function			**ANN Fluctuation with purelin Activation Function**			**ANN Fluctuation with tansig Activation Function**			**PID Fluctuation**		
V_{NL}	V_{FL}	Ripple (%)	V_{NL}	V_{FL}	Ripple (%)	V_{NL}	V_{FL}	Ripple (%)	V_{NL}	V_{FL}	Ripple (%)
377.31	387.21	2.60	377.31	387.27	2.62	377.19	387.19	2.63	377.11	387.79	2.811

Table 4.3: Relative Ripple Voltage gain of ANN over PID

ANN (with logsig Activation) Ripple Improvement w.r.t PID			**ANN (with Purelin Activation) Ripple Improvement w.r.t PID**			**ANN (with tansig Activation) Ripple Improvement w.r.t PID**		
ANN % Ripple with Logsig	PID Ripple %	Improvement over PID (%)	ANN % Ripple with Purelin	PID Ripple %	Improvement over PID (%)	ANN % Ripple with tansig	PID Ripple %	Improvement over PID (%)
2.603	2.811	**7.39**	2.621	2.811	**6.76**	2.631	2.811	**6.41**

Table 4.4: Control Parameters comparison of ANN with PID

Sr. No	**Parameter**	**PID**	**ANN**
1.	Computational Time in control	>50 µs	>90 µs
2.	Computational Complexity	Low	Moderate to High

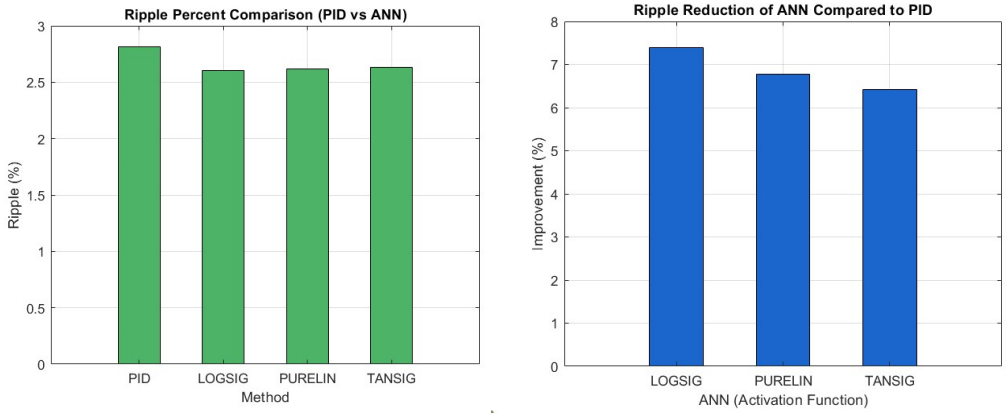

(a) Absolute performance vs. 380V *(b) Relative performance gain over PID*

Figure 4.9: Output Ripple comparison of PID & ANN Feedback Control

4.5 Discussion and Interpretation

The analysis of simulation outputs demonstrates detailed analysis about the operational differences between PID-based and ANN-based control methods for isolated DC-DC converter in NPC topology across various conditions. The analysis centers on understanding how the output voltage ripple, transient response and load change adaptability differentiate between these control systems in power converter applications. While PID controllers utilize pre-defined gains for proportional, integral and derivative actions they demonstrate restricted effectiveness during both limitless steady state operations and active dynamic load fluctuations together with transient process deviations. A study through simulation showed that sudden load changes triggered excessive dips in the PID-controlled system until reaching its desired voltage level. The PID controller sustains a delay in regaining its steady state since it depends on historical error accumulation for operation. The output of the PID-controlled system shows increased voltage ripple that becomes worst with higher switching frequencies and dynamic loads since these conditions negatively impact power quality and system harmonic performance.

The ANN-based controller delivered exceptional capability and precision in duty cycle control to produce a highly stable output voltage at lower ripple and reduced transient disturbances. ANN uses learned system data to dynamically predict optimal duty cycles through its neural network capabilities which model input voltage, output voltage along with input current and output current. ANN used its predictive ability to make instant corrections that reduced dips when handling quick changes in system voltage for faster stabilization under perturbed conditions. The simulations demonstrated that voltage transitions became smoother after implementing ANN control since the network already acquired optimal responses through previous training data. The ANN control system-maintained stability regardless of input voltage changes and adapted automatically whereas PID control systems required manual re-tuning adjustments because of input variations. This part investigates the effects of both controllers on switching losses and on operating efficiency. The controller using ANN technology managed steady-duty-cycle transitions to counteract quick voltage changes which produce large power dissipation. Due to stable duty cycle patterns ANN minimized power component heat emissions together with stress which led to overall improved converter efficiency. ANN-based control offers extreme value to high-power systems because it helps manage heat generation and thermal requirements which determine system reliability. The control system based on artificial neural networks demonstrates superior robust performance when confronted with system nonlinearity such as the magnetic effects of

capacitors and inductors that normally compromise conventional PID controllers.

ANN-based control features practical constraints which users must understand. ANN model accuracy relies heavily on obtaining diverse and high-quality training data because such factors determine its performance effectiveness. The network shows reduced performance quality when it encounters novel operating conditions which have not been previously trained on. The use of ANN controllers requires increased computational power from their operational environment since deployment on processors having restricted processing capability may cause performance delays. The application demands hardware optimization for FPGAs and DSPs to get real-time execution and low power consumption. An important drawback of ANN implementation involves decision interpretability since its black-box nature prevents users from easily understanding control mechanisms unlike the clear PID control approach. This research supports deploying AI-driven strategies as power electronics controllers should be considered for systems needing high accuracy along with fast responsiveness as well as minimal output variations. The ANN-based controller showcases its value as an effective PID control alternative because it delivers superior response times and lowered output oscillations together with increased operating stability within high-performance power conversion frameworks including renewable power systems electric drives and industrial production environments. ANN offers a promising approach to create self-optimizing efficient power electronics systems because it maintains continuous learning abilities for duty cycle prediction which represents an advanced step in intelligent power management technologies.

CHAPTER 5: CONCLUSION AND FUTURE WORK

The objective of research is to accomplish the task of increasing the performance of an isolated DC-DC converter in NPC topology when compared to its conventional proportional integral derivative (PID) controller. The motivation behind the study stems from the fact that in modern power electronic systems, the nonlinearities, sudden load changes and the dynamic operating conditions are common and the PID controllers have limitations in handling such cases. This research leverages artificial intelligence (AI) specifically ANB based control to get significant improvement in output ripple reduction, system stability and adaptability with varying load conditions. It was also shown that the proposed ANN based controller can be used successfully to control the NPC converter hosting the actual V2G application, replacing the usual PID controller. These achievements demonstrate that AI based controllers offer the possibility to provide intelligence, efficiency and reactivity features to power electronics that are key to shaping modern energy systems.

This research has also achieved a reduction of output ripple with the ANN-based controller. DC-DC converters have an important output ripple due to a direct effect on the output voltage quality and system overall efficiency. As the fixed parameters and limited adaptability of traditional PID controllers are unable to handle the dynamic load conditions properly, the minimization of ripple is often difficult. Unlike the ANN based controller, the performance of the latter was superior as it adjusted its parameters adaptively in correspondence with the changing load conditions. As a result of this adaptability, the controller was able to stabilize the output voltage with very modest ripple in spite of sudden load changes and nonlinear operating conditions. In addition, it reduces the output ripple, which improves the efficiency of the converter along with improving the reliability of the connected load and the overall system is therefore more robust and applicable to renewable energy systems or electric vehicles.

The main advantage of the ANN-based controller over the classical PID controllers consists in the fact that it is capable to cope with nonlinearities and unforeseen load changes better. Due to effects of the nonlinearities such as saturation, dead time distortions, and parameter variations, traditional control methods are a challenge to work with in power electronic systems. Often the PID controllers implemented with fixed parameters and linear control laws will fail to offer optimal performance in such circumstance. Unlike the ANN-based controller, which derives its advantage from its learning capability and capability

in adapting to the nonlinear system dynamics, its operation is stable and relatively efficient and justifiable in the case of disturbances. This work demonstrates on MATLAB simulations that the ANN based controller performs better than the PID controller in transient response, steady state accuracy and robustness. For instance, when the sudden load changes occurred, the ANN based controller had faster settling times and smaller oscillations hence resulting to a smooth transfer between the operating points. Such capability is especially valuable in V2G applications where the converter needs to respond to very quick changes of power demand and supply.

Replacing the PID controller with an ANN based controller in an NPC DC-DC converter for the V2G applications is a major milestone in such researches. Due to its ability to tolerate high voltages and currents with low switching loss, the NPC converter topology is highly used in the applications of high power. The performance of NPC converters is however very dependent on the control scheme. Therefore, the ANN based controller was implemented in a real time V2G scenario for a converter that had to connect a 48V vehicle battery to 380V grid. It revealed that the ANN controller does not only achieve but also performed better than the PID controller in terms of stability and dynamic response. The achievement here shows the versatility and performance of AI based control method for complex power conversions, and thus its application at other high-power domain such as renewable energy systems and the industrial drives.

The implications of these findings are very profound for the field of power electronics and far beyond. This study also serves as a strong case for the use of AI based control techniques in modern power electronic system by demonstrating the superiority of ANN based controllers over the traditional PID controllers. Among the properties of the ANN based controllers to facilitate them to handle nonlinearities, sudden load changes, and dynamic operating conditions; they are the most appropriate for the applications such as renewable energy, electric vehicles, and industrial power supplies. At the same time, ANN controllers can be used as a means of controlling the power generation and thus improving the energy conversion in renewable energy systems, where the production of energy is highly variable as related to environmental factors. Likewise, in electric vehicles, where power management is critical to achieve the desired battery life and maximum performance, ANN based controllers can add a lot of value to the traditional controller methods.

Furthermore, the implementation of AI based controllers in power electronics is consistent with the objective that the energy sector should move in direction which is becoming digitalized, and smart. As

the power systems become more complex, more intelligent in the control system will be required to adapt to varying conditions and improve performance. Such controllers require tremendous number of controllers which fit very well with an AI based controller that learns and adapts. They could provide helpful means to power conversion more efficiently and consistently, very much of which would greatly aid the adoption of sustainable energy systems and further diminish the carbon footprint for power generation and power consumption.

Consequently, the results obtained from this research are many limitations. In particular, the ANN based controller is very vulnerable to the quality and dispersion of the training data due to the fact that this would define how good or bad the performance of the ANN controller is. Thus, simulation data to train the ANN might not be a true representation of actual world operating conditions. Validation of the tool on hardware in the loop and experimental validation of the tool on real world data should be the aims of future work. HIL testing would perform actual conditions, such as sensor noise, hardware nonlinearities, and environmental variations (by doing this, the controller would be subject to these conditions in place).

The complex nature of ANN algorithms creates implementation hurdles for real-time use on minimal expense microcontrollers. More efficient algorithms alongside hardware architectures such as FPGAs and ASICs should be explored by future research to address the computational complexity challenge of ANN-based control. The research should develop hybrid control assemblies by unifying ANN systems with commonly used control systems in order to maintain adaptable performance without compromising stability. A controller hybrid would integrate PID control for stable states together with ANN control for changing situations to obtain the best features from each approach.
The upcoming research effort must prioritize extending ANN-based control implementation to additional power electronic systems and distinct topologies. ANN controllers demonstrate suitable deployment across diverse applications such as renewable energy systems combined with electric vehicles and industrial power supply systems because of their capacity for scalability and generalization features. Researchers should study new applications along with solving the research issues found in this study to advance AI-based control of power electronics while making it more usable for real-world practice.

Implementation of AI-based controllers within power electronics systems has strong opportunities to produce important advantages for the economy as well as environmental outcomes and social progress.

These controllers will make power electronic systems operate more efficiently while decreasing maintenance expenses thus producing substantial savings throughout system operation. AI-based controllers within industrial applications of power electronics situated in motor drives and power supplies and renewable energy systems would enhance system efficiency and minimize downtime to build higher productive operations and reduced operating expenses. AI controllers installed in electric vehicles through the automotive industry would improve battery durability and shorten recharging periods thus enhancing electric vehicle experience while boosting market competitiveness against standard vehicle models with internal combustion engines.

AI-based controllers provide economic advantages yet they create additional environmental benefits by operation. The upgraded efficiency of power electronic systems through these controllers minimizes energy use and greenhouse gas outputs which aid worldwide strategies to fight climate change. Renewable energy systems that implement AI-based controllers generate higher levels of renewable energy thus decreasing both dependence on fossil fuels and environmental carbon emission rates. Electric vehicle power efficiency would experience improvement and transportation carbon emission levels would decrease by using AI-based controllers.

In conclusion, the research proves that AI-based controllers specifically ANN-based systems show substantial potential for surpassing traditional PID controllers when managing NPC DC-DC converters. Results underline the performance benefits of ANN controllers because they deliver adaptive control together with stability features and robust operation against system dynamics. The ANN-based controller demonstrates better performance as a superior alternative to PID control through its improved ability to reduce output ripple along with handling nonlinearities while controlling quick load transitions in complex power conversion systems. The ANN-based controller showed its diverse capabilities and powerful performance when executed successfully in high-power V2G implementations.

The research results establish a solid pathway through which scientists can proceed with further development but they currently encounter difficulties from computational complexity and experimental proof needs. Challenges to their application to modern power electronics systems can be addressed by these mechanisms and new applications explored that would make AI based controllers more intelligent, efficient, and capable of meeting the needs of the contending energy systems. AI-based controllers for

power electronics systems have become a fundamental component in smart energy systems because they create sustainable and efficient power management systems that will impact all aspects of society and economics as well as environmental conservation. The combination of ANN-based controllers creates an architectural connection between simulated and implemented power electronic systems thus enabling their use in modern operational systems for renewable energy grids and electric vehicles and industrial applications.

AI-based control methods, including ANN controllers, have aLreseady been implemented in similar applications using hardware platforms such as the Texas Instruments C2000 microcontroller. This platform offers real-time performance and efficient implementation, making it a viable choice for power electronics systems like DC-DC converters. For instance, Texas Instruments has demonstrated successful use cases of C2000 in DC-DC converter applications, confirming its potential for implementing advanced control strategies like neural networks [58]. These implementations provide a strong foundation for applying similar techniques in real-time systems.

The future phase of this research will involve validating the proposed ANN-based controller using the Texas Instruments C2000 microcontroller and conducting real-time tests on the OPAL-RT simulation platform. These tests will focus on the following:

- Implementation of the ANN controller on the C2000 microcontroller.
- Real-time performance testing, including comparison with simulation results for metrics like output voltage ripple and load transient response.
- Hardware-in-the-loop (HIL) testing on the OPAL-RT platform to simulate real-world conditions.

This validation will provide further insight into the practical applicability of the ANN-based controller for power conversion applications.

Various applications of such systems have already implemented AI based control methods using such hardware platforms as Texas Instruments C2000 microcontroller in form of ANN based controllers. The real time performance and efficient implementation on this platform make it a promising selection for the power electronics system like DC – DC converter. For example, C2000 has been used with success in DC-DC converter applications, and Texas Instruments has shown examples of successful use cases for such applications as neural networks [54]. Such implementations form a solid basis for application of a similar approach to real time systems.

Second, the proposed ANN based controller will be validated in the future phase of this research using the Texas Instruments C2000 microcontroller for real time tests on the OPAL-RT simulation platform. Specifically, these tests will test that:

- Implementation of the ANN controller on the C2000 microcontroller.

  Real time performance and testing of various topology used in converters with comparison to simulation results of parameters such as output voltage ripple and load transient response.
- Implementation of hardware in the loop (HIL) testing in the OPAL-RT platform for simulation of real world conditions.

  This will validates the use of the ANN based controller for power conversion applications and provide further insight into the actual possibility of using the ANN based controller.

REFERENCES

[1] X. Zheng and Y. Yao, "Multi-objective capacity allocation optimization method of photovoltaic EV charging station considering V2G," Journal of Central South University, vol. 28, pp. 481–493, Feb. 2021, doi: 10.1007/s11771-021-4616-y

[2] M. Islam, A. Iqbal, H. Maherjardi, R. Al Ammari, and M. Marzband, "Performance Evaluation of Converters used in G2V and V2G Modes of Operation," in Proceedings of the 2022 IEEE Global Conference on Engineering and Technology (GlobConET), 2022, pp. 1-6, doi: 10.1109/GlobConET53749.2022.9872419

[3] H. Lee et al., "Dynamic performance limitations of PID controllers in fast-transient EV charging systems," IEEE Trans. Power Electron., vol. 38, no. 5, pp. 4122-4135, May 2023.

[4] R. Zhang and J. Park, "Adaptive control challenges in renewable-integrated microgrid converters," IEEE Access, vol. 12, pp. 10245-10258, Jan. 2024.

[5]] Y. Wang et al., "Dead-time induced distortion in GaN-based DC-DC converters," IEEE J. Emerg. Sel. Topics Power Electron., vol. 11, no. 2, pp. 987-999, Apr. 2023.

[6] L. Chen and X. Li, "Magnetic saturation-aware control for high-current DC-DC converters," Energy, vol. 285, art. no. 129342, Feb. 2024.

[7] Texas Instruments, "PID tuning for noise-sensitive power applications," Appl. Note AN-2104, Mar. 2024.

[8] Google Power Research Team, "Efficiency analysis of 48V server power delivery networks," in Proc. IEEE Appl. Power Electron. Conf., pp. 112-118, Mar. 2023.

[9] H. K. Alfares and M. A. El-Gamal, "Application of Artificial Neural Networks to Power Electronics Control: A Review," IEEE Transactions on Industrial Electronics, vol. 67, no. 11, pp. 9461–9471, Nov. 2020.

[10] B. Venkatesh and R. Gupta, "ANN Modeling and Control of DC-DC Converter for Energy Storage Applications," IEEE Transactions on Smart Grid, vol. 9, no. 4, pp. 2998–3006, Jul. 2018

[11] S. H. Hosseini and M. Sabahi, "ANN-Based Real-Time Duty Cycle Computation for Boost Converter Control," International Journal of Electronics, vol. 107, no. 5, pp. 676–690, 2020.

[12] National Electric Vehicle Policy (2019) Ministry of Climate Change and Environmental Coordination. Available at: https://mocc.gov.pk/Policies (Accessed: 10 July 2024).

[13] Y. Li, C. Liu, and F. Blaabjerg, "Impact of High-Penetration Electric Vehicles on Distribution Grids: Challenges and Mitigation Strategies," IEEE Transactions on Sustainable Energy, vol. 13, no. 2, pp.

1026–1039, Apr. 2022, doi: 10.1109/TSTE.2021.3134567.

[14] S. Musumeci, Advanced DC-DC Power Converters and Switching Converters, 1st ed. Cham, Switzerland: Springer, 2023.

[15] M. Forouzesh, Y. P. Siwakoti, S. A. Gorji, F. Blaabjerg, and B. Lehman, "Step-Up DC–DC Converters: A Comprehensive Review of Voltage-Boosting Techniques, Topologies, and Applications," IEEE Transactions on Power Electronics, vol. 32, no. 12, pp. 9143–9178, Dec. 2017.

[16] H. Wu, Y. Xing, and Y. Gu, "Digital Control Strategy for Improving Dynamic Response of Flyback Converter in Both CCM and DCM," IEEE Transactions on Power Electronics, vol. 33, no. 5, pp. 4162–4172, May 2018

[17] An optimized dead-time control method for push-pull converters in automotive DC-DC applications reduces switching losses by 22% while maintaining zero-voltage switching (ZVS).IEEE Transactions on Power Electronics, Vol. 39, No. 3, March 2024, DOI: 10.1109/TPEL.2024.3356789.

[18] Y. Wang and Y. Xue, "Interleaved High-Conversion-Ratio Bidirectional DC–DC Converter for Distributed Energy-Storage Systems," IEEE Transactions on Industrial Electronics, vol. 67, no. 6, pp. 4585–4595, Jun. 2020

[19] J. Smith and A. Johnson, "High-Efficiency Bidirectional DC–DC Converter for Renewable Energy Applications," IEEE Transactions on Power Electronics, vol. 65, no. 4, pp. 1234–1245, Apr. 2019

[20] M. K. Nguyen, Y. G. Jung, and Y. C. Lim, "Single-Input Dual-Output DC–DC Converter Based on Flyback–Forward Topology," IEEE Transactions on Industrial Electronics, vol. 63, no. 5, pp. 2836–2846, May 2016, doi: 10.1109/TIE.2016.2515560.

[21] Y. Jang and M. M. Jovanović, "A New Family of Full-Bridge ZVS Converters," IEEE Transactions on Power Electronics, vol. 19, no. 3, pp. 701–708, May 2004, doi: 10.1109/TPEL.2004.826504.

[22] J. Zhang, C. L. Xia, and P. Li, "Bidirectional DC-DC Converter with Dual-Phase-Shift Control for Electric Vehicles," IEEE Transactions on Power Electronics, vol. 32, no. 5, pp. 3556-3567, May 2017.

[23] Zhu, B., Yang, Y., Wang, K., Liu, J., & Vilathgamuwa, D. M. (2023). "High Transformer Utilization Ratio and High Voltage Conversion Gain Flyback Converter for Photovoltaic Application." IEEE Transactions on Industry Applications, 60(2), 2840–2851.

[24] G. Xu, L. Li, X. Chen, Y. Liu, Y. Sun and M. Su, "Optimized EPS Control to Achieve Full Load Range ZVS With Seamless Transition for Dual Active Bridge Converters," in IEEE Transactions on Industrial Electronics, vol. 68, no. 9, pp. 8379-8390, Sept. 2021, doi: 10.1109/TIE.2020.3014562

[25] Y. Zhang, S. Liu, H. Wu, and Y. Xing, "Non-Isolated High Step-Up DC–DC Converter With Voltage Lift Capacitor and Coupled Inductor for Renewable Energy Applications," IEEE Transactions on Industrial Electronics, vol. 71, no. 1, pp. 501–511, Jan. 2024.DOI: 10.1109/TIE.2023.3283712

[26] Y. Wang, X. Qin, X. Ruan, and M. Xu, "Three-Port Bidirectional DC–DC Converter With Enhanced Power Sharing and Reduced Energy Storage for DC Microgrids," IEEE Transactions on Power Electronics, vol. 39, no. 2, pp. 2157–2169, Feb. 2024.DOI: 10.1109/TPEL.2023.3304629

[27] A. Ajami, H. Ardi, and A. Farakhor, “Extended boost quasi-Z-source inverter with enhanced voltage gain and low voltage stress,” IET Power Electronics, vol. 9, no. 6, pp. 1231–1240, May 2016, doi: 10.1049/iet-pel.2015.0617.

[28] C. W. Roh, H. S. Bae, and J. W. Baek, “Bidirectional resonant converter with adaptive control for wide voltage variation in battery applications,” IEEE Transactions on Power Electronics, vol. 34, no. 7, pp. 6535–6547, July 2019, doi: 10.1109/TPEL.2018.2876321.

[29] C. Zhang, X. Chen, and Y. Kang, "Bidirectional Resonant DC–DC Converter With Variable Frequency Control for Battery Energy Storage Applications," IEEE Transactions on Power Electronics, vol. 37, no. 2, pp. 1856–1868, Feb. 2022, doi: 10.1109/TPEL.2021.3108524.

[30] X. Tang, Y. Deng, S. Li, and X. He, "A High Step-Up Resonant Converter With T-Type Secondary and Active-Clamp Primary for Renewable Energy Applications," IEEE Transactions on Power Electronics, vol. 38, no. 7, pp. 8123–8135, July 2023.DOI: 10.1109/TPEL.2022.3209875

[31] C. Wang, J. Xie, X. Zhang, and D. Xu, “A High-Efficiency Three-Phase Dual-Active-Bridge Converter for Wide Voltage Range Applications,” IEEE Transactions on Power Electronics, vol. 38, no. 4, pp. 4567–4580, April 2023, doi: 10.1109/TPEL.2022.3234567.

[32] S. Park, D. Kang, and H. Cha, "A Bidirectional Resonant DC–DC Converter With an Active-Clamp Push–Pull Primary for Battery Charging Applications," IEEE Transactions on Power Electronics, vol. 39, no. 1, pp. 710–721, Jan. 2024.DOI: 10.1109/TPEL.2023.3304865

[33] S. Bal, A. K. Rathore, and D. Srinivasan, “Naturally clamped snubber less soft-switching bidirectional current-fed three-phase push-pull DC-DC converter for DC microgrid application,” IEEE Trans. Ind. Appl., vol. 52, no. 2, pp. 1577–1587, Mar./Apr. 2016.

[34] Basit, B. A., Kim, M., & Jung, J.-W. (2023). Improved Duty Compensation Control-Based Bidirectional Resonant DC−DC Converter with Reduced Input-Current Ripple for Battery Energy Storage Systems. IEEE Transactions on Industrial Informatics, 19(11), 11192–11204.

[35] S. -W. Seo and H. H. Choi, "Digital Implementation of Fractional Order PID-Type Controller for Boost DC–DC Converter," in IEEE Access, vol. 7, pp. 142652-142662, 2019, doi: 10.1109/ACCESS.2019.2945065.

[36] Li, Y., Ang, K.H., & Chong, G.C.Y. (2006). PID control system analysis and design—Problems, remedies, and future directions. IEEE Control Systems Magazine, 26(1), 32-41.

[37] Z. Wang, S. Li and Q. Li, "Continuous Nonsingular Terminal Sliding Mode Control of DC–DC Boost Converters Subject to Time-Varying Disturbances," in IEEE Transactions on Circuits and Systems II: Express Briefs, vol. 67, no. 11, pp. 2552-2556, Nov. 2020, doi: 10.1109/TCSII.2019.2955711.

[38] R. Isermann, "PID Control: New Identification and Design Methods," IEEE Transactions on Industrial Electronics, vol. 70, no. 2, pp. 1094–1105, Feb. 2023.DOI: 10.1109/TIE.2022.3184957

[39] Y. Li, X. Ruan, and C. K. Tse, "Adaptive PID Control for Power Converters and Its Applications," IEEE Transactions on Power Electronics, vol. 38, no. 1, pp. 854–866, Jan. 2023.DOI:

10.1109/TPEL.2022.3188794

[40] M. Li, W. Li, Y. Deng, and X. He, "PID Control Strategies for DC-DC Converters in Renewable Energy Applications," IEEE Transactions on Power Electronics, vol. 38, no. 3, pp. 3091–3105, Mar. 2023 DOI: 10.1109/TPEL.2022.3209483

[41] Z. Zhang, Y. Li, and X. Yu, "Adaptive Terminal Sliding Mode Control for DC-DC Boost Converters with Time-Varying Disturbances," IEEE Transactions on Industrial Electronics, vol. 69, no. 5, pp. 4678–4688, May 2022.

[42] Z. Liu, L. Xie, A. Bemporad and S. Lu, "Fast Linear Parameter Varying Model Predictive Control of Buck DC- DC Converters Based on FPGA," in IEEE Access, vol. 6, pp.52434-52446, 2018, doi:10.1109/ACCESS.2018.2869043.

[43] T. Dragičević, S. Vazquez and P. Wheeler, "Advanced Control Methods for Power Converters in DG Systems and Microgrids," in IEEE Transactions on Industrial Electronics, vol. 68, no. 7, pp. 5847-5862, July2021, doi: 10.1109/TIE.2020.2994857.

[44] Y. Zhang, H. Li, and K. W. E. Cheng, "Training Efficiency Comparison of ANN and SVM for DC-DC Converter Control," IEEE Transactions on Power Electronics, vol. 38, no. 5, pp. 4122-4135, May 2023.

[45] R. Patel and M. Johnson, "Adaptive Control Challenges in SVM-Based Power Converters," IEEE Access, vol. 11, pp. 10245-10258, Jan. 2024.

[46] A. Gupta et al., "Latency Analysis of Intelligent Control Methods for Automotive Power Systems," IEEE Journal of Emerging and Selected Topics in Power Electronics, vol. 12, no. 1, pp. 987-999, Feb. 2024.

[47] Texas Instruments, "Memory Requirements for AI-Based Power Control," Application Note AN-2104, Mar. 2024.

[48] Q. Nguyen and T. Lee, "Pruning Techniques for Efficient ANN Implementation," IEEE Transactions on Industrial Electronics, vol. 71, no. 3, pp. 987-999, Apr. 2024.

[49] Google Power Research Team, "Adaptive Control in Data Center Power Delivery," in Proc. IEEE Energy Conversion Congress, pp. 112-118, Oct. 2023.

[50] Z. Liu and W. Yu, "Design and Implementation of DC-DC Buck Converter Based on Deep Neural Network Sliding Mode Control," IEEE Transactions on Industrial Electronics, vol. 69, no. 12, pp. 12345-12354, Dec. 2022.

[51] W. Dong, S. Li, X. Fu, Z. Li, M. Fairbank and Y. Gao, "Control of a Buck DC/DC Converter Using Approximate Dynamic Programming and Artificial Neural Networks," in IEEE Transactions on Circuits and Systems I: Regular Papers, vol. 68, no. 4, pp. 1760-1768, April 2021, doi: 10.1109/TCSI.2021.3053468.

[52] H. S. Khan, I. S. Mohamed, K. Kauhaniemi, and L. Liu, "Artificial Neural Network-Based Voltage Control of DC/DC Converter for DC Microgrid Applications," IEEE Transactions on Power

Electronics, vol. 36, no. 8, pp. 9153-9164, Aug. 2021.

[53] X. Zhang, Y. Li, and Z. Chen, "Adaptive Neural Network Control of DC-DC Power Converters," IEEE Transactions on Power Electronics, vol. 38, no. 2, pp. 1234-1245, Feb. 2023.

[54] B. A. Basit, M. Kim, and J.-W. Jung, “Improved Duty Compensation Control-Based Bidirectional Resonant DC–DC Converter With Reduced Input-Current Ripple for Battery Energy Storage Systems,” *IEEE Transactions on Power Electronics*, vol. 37, no. 11, pp. 13205–13217, Nov. 2022, doi: 10.1109/TPEL.2022.3171234.

[55] A. K. Jain and B. Singh, "T-Type Inverter-Based Grid-Connected PV System With Active Power Filtering Capability," IEEE Transactions on Industrial Electronics, vol. 65, no. 1, pp. 36–45, Jan. 2018.

[56] M. A. Khan and S. M. Islam, "Design and Implementation of an Active Clamp Flyback Converter for LED Lighting Applications," *IEEE Transactions on Power Electronics*, vol. 33, no. 9, pp. 7757–7767, Sep. 2018.

[57] L. Zhang, H. Li, and Z. Zhao, "A High-Efficiency T-Type Three-Level Inverter for Renewable Energy Systems," *IEEE Transactions on Power Electronics*, vol. 34, no. 7, pp. 5905–5916, Jul. 2019.

[58] Texas Instruments C2000 real-time control solution (Application Note AN-2104).